Please cite this article in press as: Unsworth et al., Rethinking marine restoration permitting to urgently advance efforts, Cell Reports Sustainability (2025), https://doi.org/10.1016/j.crsus.2025.100526

Cell Reports Sustainability

CellPress
OPEN ACCESS

Perspective

Rethinking marine restoration permitting to urgently advance efforts

Richard K.F. Unsworth,[1,2,*] Michael Sweet,[4] Laura L. Govers,[5,6] Sophie von der Heyden,[7] Adriana Vergés,[8] Daniel A. Friess,[9] Benjamin L.H. Jones,[2] Margaux A.A. Monfared,[10] Rune C. Steinfurth,[11] Jose M. Fariñas-Franco,[12] Leanne C. Cullen-Unsworth,[2] Timi L. Banke,[11] Fiona Tomas,[13] Bowdoin W. Lusk,[14] Anouska F. Mendzil,[1,2] Alison J. Debney,[15] William G. Sanderson,[16] Esther Thomsen,[17] Joanne Preston,[18] Elizabeth A. Lacey,[2] Kristina Boerder,[19] Rowana Walton,[20] Tali Vadi,[21] Jen Brand,[20] and Maike Paul[3]

[1]Seagrass Ecosystem Research Group, Swansea University, Singleton Park, Swansea SA2 8PP, UK
[2]Project Seagrass, Unit 1 Garth Drive, Brackla Industrial Estate, Bridgend CF31 2AQ, UK
[3]Leibniz University Hannover, Ludwig Franzius Institute of Hydraulic, Estuarine and Coastal Engineering, Nienburger Str. 4, 30167 Hannover, Germany
[4]Aquatic Research Facility, Nature-Based Solutions Research Centre, University of Derby, Derby, UK
[5]Conservation Ecology Group, Groningen Institute for Evolutionary Life Sciences (GELIFES), University of Groningen, Groningen, the Netherlands
[6]Department of Coastal Sciences, Royal Netherlands Institute for Sea Research (NIOZ), Texel, the Netherlands
[7]Department of Botany and Zoology, Stellenbosch University, Private Bag X1, Stellenbosch 7599, South Africa
[8]Centre for Marine Science & Innovation, School of Biological, Earth & Environmental Sciences, UNSW Sydney, Kensington, NSW 2052, Australia
[9]Department of Earth and Environmental Sciences, Tulane University, New Orleans, LA 70118, USA
[10]Blue Pangolin Consulting Ltd., 54 South Worple Way, London SW14 8PB, UK
[11]Department of Biology, University of Southern Denmark, Campusvej 55, 5230 Odense, Denmark
[12]Department of Natural Resources and the Environment, Marine and Freshwater Research Centre, Atlantic Technological University, Galway, Ireland
[13]Instituto Mediterráneo de Estudios Avanzados (CSIC-UIB), C/Miquel Marques 21, Islas Baleares, 07190 Esporles, Spain
[14]Virginia Coast Reserve, The Nature Conservancy, Nassawadox, VA 23413, USA
[15]Conservation & Policy, Zoological Society of London (ZSL), Regent's Park, London NQ1 4RY, UK
[16]Institute of Life and Earth Sciences, School of Energy, Geoscience, Infrastructure and Society, Heriot-Watt University, Edinburgh EH14 4AS, UK
[17]Marine Evolutionary Ecology, GEOMAR Helmholtz Centre for Ocean Research Kiel, Wischhofstraße 1-3, Kiel, Germany
[18]Institute of Marine Sciences, School of the Environment and Life Sciences, University of Portsmouth, Portsmouth PO4 9LY, UK
[19]Future of Marine Ecosystems research lab, Dalhousie University, 6283 Alumni Crescent, Halifax, NS B3H 4R2, Canada
[20]United Nations World Conservation Monitoring Centre, Cambridge, UK
[21]Coral Restoration Consortium, Brooklyn, NY, USA
*Correspondence: r.k.f.unsworth@swansea.ac.uk
https://doi.org/10.1016/j.crsus.2025.100526

SUMMARY

Marine biodiversity is rapidly declining, necessitating global political and financial solutions to prioritize habitat restoration in a "blue revolution." However, marine and coastal restoration faces major technical, logistical, and resource challenges that are exacerbated by climate change, which must be urgently addressed. Unlike terrestrial restoration, marine efforts lack a long history or well-established methods, resulting in potentially high failure rates and a pressing need for innovation. As scientists and practitioners, we argue that scaling marine and coastal restoration requires policy reform, scientific advancement, and more adaptive regulatory frameworks. Current approaches are constrained by unrealistic ecological baselines and outdated assumptions about environmental stability. Licensing must move beyond recreating past habitats and instead support resilient ecosystems, ecological connectivity, and future colonization pathways. We need to rethink restoration for a changing world, guided by flexible systems that embrace uncertainty, integrate new technologies, and prioritize long-term coastal resilience over short-term fixes.

INTRODUCTION

All available measures of the state of the ocean and coasts indicate a crisis. Marine biodiversity is in steep decline.[1] Coral reefs are facing critical tipping points,[2] and the seas are increasingly becoming devoid of top predators.[3] Ecosystems are changing or disappearing. Globally, we have lost at least 20% of seagrass meadows,[4] over 35% of mangrove forests,[5] and up to 50% of

Please cite this article in press as: Unsworth et al., Rethinking marine restoration permitting to urgently advance efforts, Cell Reports Sustainability (2025), https://doi.org/10.1016/j.crsus.2025.100526

saltmarshes.[6] Halting the widespread degradation while restoring marine and coastal life is essential for sustaining human life and planetary health.[7]

We are now 4 years into the United Nations (UN) Decade of Ecosystem Restoration and are beginning to see a movement for change that (cl)aims to prioritize marine restoration.[8] The Kunming-Montreal Global Biodiversity Framework (GBF) has set an ambitious target: to restore 30% of all degraded ecosystems, including coastal and marine ecosystems such as mangrove forests, coral and shellfish reefs, and seagrass meadows, by 2030.[9] The European Union (EU) has enacted legally binding targets to restore degraded habitats under nature restoration regulation.[10] On the global stage, ambitious coral reef, seagrass, saltmarsh, and mangrove breakthrough funds are being launched, potentially raising billions for restoration and regeneration practices.[11] Does this signal that marine and coastal restoration has finally reached a pivotal turning point?

The timing is auspicious for the large-scale restoration of marine and coastal life.[7,12,13] Like terrestrial systems, marine and coastal restoration interventions such as seagrass and mangrove planting have been found to be effective over large spatial expanses (1,000s–100,000s ha). They persist for decades, rapidly expand in size, can be cost-effective, and generate significant social and economic benefits.[14] There is also a rapidly increasing interest from the corporate sector to fund marine projects that support environmental credits, driving potential future investments into restoration.[15]

However, despite the promising outlook, marine and coastal restoration is challenging. There is a high demand for innovative tools and methods, but knowledge lags behind terrestrial systems due to the relatively young age of the discipline.[16] It also requires a tolerance of greater risk and failures during pioneering and/or development phases as we gather data to inform and increase the efficacy of future efforts. Furthermore, restoration efforts are hindered by numerous technical, logistical, and resource challenges that urgently require resolution before global restoration commitments can be achieved at the necessary rate and scale. These can include prohibitive costs, complex governance, socio-cultural conflicts, political pushback and/or unwillingness to act, methodological challenges, and significant scientific knowledge gaps, which create bottlenecks to advancing marine and coastal restoration.

We, as a group of 25 scientists and practitioners working on marine restoration across six ecosystems in 18 countries, argue for an urgent and major cultural shift in how restoration of the world's oceans is both approached scientifically and regulated governmentally. This shift is essential to ensure that marine restoration activities pursue long-term sustainability while engaging and benefiting people.[17] Marine and coastal restoration is in its infancy and therefore lends itself to an exploratory research approach, while also providing an opportunity for robust scientific advancements using novel approaches and techniques.

Recent technological advances have introduced new tools and methods for monitoring and understanding marine and coastal ecosystems but have also brought about unique legal, institutional, and regulatory challenges that necessitate cooperation across local, national, and international scales.[18,19] Legislation and regulations intended to protect the environment can inadvertently hinder restoration efforts through extensive delays, disproportionate costs, and bureaucratic barriers—sometimes leading to suboptimal outcomes or project abandonment (see Figure 1). Therefore, we discuss how (and why) such legislation and regulations can lead to unintended consequences for restoration, using a series of international case studies (Boxes 1, 2, and 3). We outline how regulatory and licensing solutions that facilitate restoration and habitat creation can support a smoother and more scientifically robust workflow, from identifying the need for restoration to implementing restoration activities, thereby contributing to achieving national and international environmental policy targets.

MARINE RESTORATION IS IN ITS INFANCY

The restoration of marine and coastal ecosystems is a relatively young field that has mostly developed within the last 50 years. While the first recorded evidence of kelp restoration dates back to over 300 years ago,[28] and the first oyster and seagrass restoration projects began around 90 years ago,[29] sustained investment into the science underpinning this work has only begun to take shape in recent decades.[14] Managed realignment projects, facilitating saltmarsh recovery, and mangrove planting have the longest history of scaled-up activity.[30,31] Coral reef restoration developed fairly rapidly with strong investment but only reached an extensive level in the 1970s due to the advancements in SCUBA.[11]

However, with infancy comes responsibility and necessity—we can and should be accountable for all restoration applications, learning from both failures and successes. This aligns with the principles of responsible innovation and research.[32] "Failure" (i.e., the First Attempt In Learning [FAIL]) in marine restoration projects and experiments is likely very high but often goes unreported.[33,34] These failures are not necessarily due to restoration being unviable but are caused by the low level of development of the science. Many techniques utilized are still novel and unproven but are developing rapidly, and innovation remains critical to the field's expansion.[35]

Learning from failure must be implemented alongside consistent and transparent monitoring, evaluation, and reporting systems that enable adaptive learning and knowledge exchange (key information about species, methods, locations, and reports describing project outcomes) across the restoration community. A database dedicated to reporting marine restoration activities does exist in Australia and New Zealand.[36] Key organizations and networks in the seagrass and mangrove restoration communities have now launched tools (SeagrassRestorer.org and GlobalMangroveWatch.org), providing opportunities for practitioners and the wider community to get involved; however, these need wider uptake and involvement from the restoration community.

Conducting successful restoration is not simple. It requires a high level of scientific expertise, as well as innovative and adaptable projects that address the inherent uncertainties of current methodologies and the challenges imposed by a changing climate. Unlike the management of terrestrial fauna through plantings of flora, which have been ingrained in human culture

Please cite this article in press as: Unsworth et al., Rethinking marine restoration permitting to urgently advance efforts, Cell Reports Sustainability (2025), https://doi.org/10.1016/j.crsus.2025.100526

CellPress
OPEN ACCESS

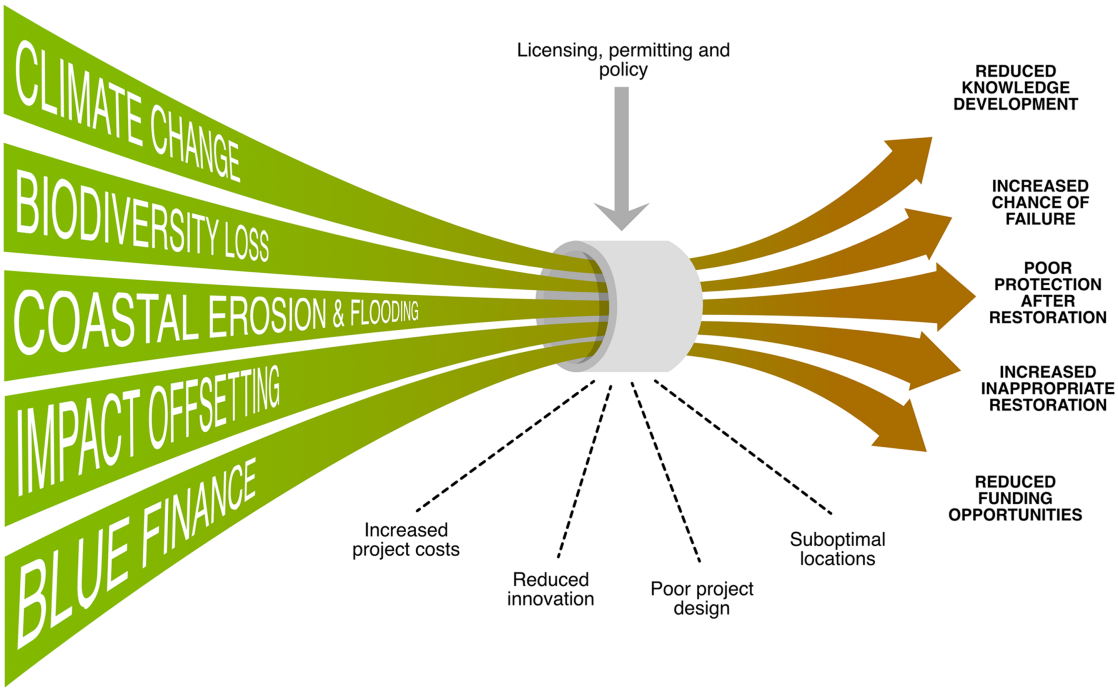

Figure 1. The consequences of increasing bottlenecks to marine and coastal restoration activity that are preventing the delivery of such projects at scale

and history for millennia, marine and coastal restoration lacks this extensive historical development.[37] However, time is running out for ocean and coastal ecosystems on planet earth,[38] and the cost of inaction is high.[39] In the context of urgency, there are also a series of arguments for the use of proactive (reduce the chance of loss before it happens) rather than just reactive (after the loss) restoration. As per all restoration programs, planting or creating habitat is no substitute for management actions to prevent loss in the first place.[40]

LEARNING TO EMBRACE NOVELTY

The expectation that reliable marine and coastal restoration solutions can be developed within the remaining 5 years of the UN Decades on Ocean and Ecosystem Restoration is optimistic at best. While there are many emerging examples of successful marine and coastal restoration project outcomes,[14] marine and coastal restoration, especially in the presence of knowledge gaps, takes time. Results need to be considered over extended periods, sometimes decades. This is exacerbated by failures that often relate to limited understanding of a particular process. Achieving large-scale restoration to meet ambitious local and international targets will require licensing and regulation that support and facilitate innovation and cooperation.

For restoration to be long-lasting, scientists need the flexibility[41] to test ecological restoration approaches, which include bionovelty[42] (see Table 1). Bionovelty includes assisted evolution, restorative aquaculture, assisted gene flow, the use of probiotics, the use of non-native species (e.g., Pacific oysters), manufactured habitats, methods, and translocations.[43] While we recognize that these novel approaches have various ethical considerations important to decision-making, exploring these issues is beyond the scope of this paper.[44]

Species that are transported by human activity, intentionally or unintentionally, into regions where they do not naturally occur are referred to as "non-native," "alien," "invasive," or "introduced" species.[45] The presence of invasive species often constrains marine and coastal restoration. Their movement may be prohibited, and restoration projects may be restricted to prevent further spread, thereby discouraging activity in areas already dominated by them. Under rapid climate change, however, eradication of widespread, dominant invaders is increasingly unrealistic. This does not imply abandoning control of new or localized invasions, which remains essential,[46] nor overlooking the negative impacts invasives can have on native biota, for instance, *Sonneratia apetala* outcompeting native flora in China[47] or the spread of *Spartina alterniflora* in tidal marshes.[48]

While many invasive species fail to survive in new environments, some establish and outcompete native species or habitats. In parts of the world, some invasive species have spread well beyond the point of biological control and now form a major component of local flora and fauna. This has led to the rise of ecological novelty, or *novel ecosystems*, where species assemblages and functions lack historical precedent.[49] Examples include the creation of novel biogenic or foundation habitats by species such as the American slipper limpet *Crepidula fornicata*,[50] cordgrass *Spartina spp.*, the Pacific oyster *Magallana gigas*, and the Japanese wireweed *Sargassum muticum*.[51]

Where invasives are firmly established and beyond control, restoration efforts could benefit from harnessing their ecological

Please cite this article in press as: Unsworth et al., Rethinking marine restoration permitting to urgently advance efforts, Cell Reports Sustainability (2025), https://doi.org/10.1016/j.crsus.2025.100526

Box 1. Restoration of seaweed in MPAs in Australia

Restoration of seaweed in Australia (Photo Credit: Tom Burd and Adriana Vergés) Efforts to restore crayweed forests along Sydney's coastline involve attaching reproductive seaweeds to temporary mats on the seafloor to promote natural establishment.[20] However, permitting restrictions have limited deployments inside MPAs in Sydney, Australia, forcing most work over the past decade into unprotected areas where conditions may be less advantageous for restoration. These restrictions forfeit potential ecological advantages of MPAs demonstrated around the world. In many seaweed ecosystems, fishing bans can trigger trophic cascades, boost predators, reduce herbivores, and promote seaweed recovery.[21] Marine protection can also enhance kelp resilience to marine heatwaves[22] and deliver social benefits, including enhanced community stewardship and cultural connection.[23,24] Indeed, global examples show that protection and seaweed restoration can be highly complementary. For example, sea urchin removal in Mediterranean no-take zones has restored seaweed beds,[25] while in Port Phillip Bay (Australia), combining urchin harvests with kelp seeding inside MPAs is also driving effective recovery.[26]

traits rather than treating them solely as obstacles. Instead, their potential ecological roles may need reassessment, for example, as facilitators of other species' recovery or as providers of habitat.[52] If invasive species possess traits that deliver desirable ecosystem functions or services,[53] enhance resilience to environmental change, or improve ecosystem stability (e.g., via high water filtration rates), they may merit integration into restoration strategies.[54] Notably, restrictions on restoration often contrast with historical and ongoing fisheries practices. For example, oyster restoration is tightly regulated due to disease and genetic concerns, yet fisheries have routinely transported bivalves across Europe for centuries.[55] Meanwhile, Pacific oysters, though globally invasive, can provide multiple ecosystem services in their non-native ranges.[56]

Coastal ecosystems are frequently altered beyond all recognition due to anthropogenic change, with the 1953 Netherlands Delta Plan to build dikes and dams across Europe's biggest delta as such an example.[57] The rapid expansion of megacities in SE Asia is also resulting in coastal land use change,[58] on top of extensive and progressing shoreline alteration for aquaculture.[59] These locations are characterized by continual disturbance (e.g., maintenance dredging and shipping), which in turn results in reduced connectivity and the complete elimination of entire ecological groups. In such areas, there is often no or limited recovery capacity, and ecological restoration potential is extremely limited by the availability of biological material. In such cases, assisted gene flow or assisted colonization are becoming increasingly essential and therefore urgently require

Please cite this article in press as: Unsworth et al., Rethinking marine restoration permitting to urgently advance efforts, Cell Reports Sustainability (2025), https://doi.org/10.1016/j.crsus.2025.100526

CellPress
OPEN ACCESS

Box 2. Seagrass restoration in England

Intertidal seagrass restoration activities in the Isle of Wight, England (Photo Credit: Anouska Mendzil) Seagrass restoration in England faces major challenges due to inconsistent monitoring, management, and licensing. Most projects use a seed-based approach, often sourcing from unsuitable provenances due to licensing authorities dictating donor meadows without considering environmental compatibility, undermining restoration efforts. Bureaucratic systems further restrict access to suitable seed sources: critical regional meadows are heavily protected, while other viable meadows remain unmapped and overlooked. NGOs and charities are also increasingly tasked with providing data for designated site assessments (e.g., site of special scientific interest and MPAs) without financial support, despite gaps in evidence on meadow condition and inconsistent survey timelines. Licensing delays compound the problem, often taking 6–12 months or longer, with multiple permits required across multiple agencies, slowing delivery, increasing costs, and reducing project scale.

Protected species regulations create additional barriers. Under the Wildlife and Countryside Act (1981), seahorse habitat is protected, yet while damaging activities continue in seagrass, restoration and scientific surveys face restrictive licensing. Definitions of meadow "health" used to

(continued on next page)

CellPress
OPEN ACCESS

Cell Reports Sustainability
Perspective

regulate seed collection lack a scientific basis, hindering restoration by preventing collection from suitable donor sites. Restoration is largely led by NGOs, charities, and research groups, funded by private and charitable donations, rather than the government. Rising licensing costs, band fees, annual increases, and advisory charges make small-scale projects unfeasible while favoring large developers (who aren't involved in seagrass restoration or don't have the appropriate capacity). Introducing zero-cost licensing bands or exemptions for non-profit, environmentally beneficial projects would reduce financial barriers, allowing more funds to be directed toward habitat recovery without weakening environmental safeguards.

serious consideration by licensing authorities (both nationally and internationally).

Climate change is rapidly influencing how we consider marine restoration. Even if global temperatures were maintained within the 1.5°C target of the Paris Climate Agreement, marine and coastal ecosystems would face substantial risks.[60] As global temperatures rapidly increase, the ecology of the planet is undeniably shifting at an equally rapid rate.[61] The success of "business as usual" conservation, restoration, and legislative procedures becomes increasingly unrealistic with each heating event. This has resulted in calls from terrestrial restoration initiatives in Australia to embed climate change in ecological restoration law and practice.[62] Therefore, established principles of ecological restoration need to consider and ensure "future proofing" is undertaken.[63] Instead of simply recreating past ecosystems, efforts should be made to facilitate resilient ecosystems for the future.[41]

To get ahead of climate change, we need to go beyond preservationist approaches by including strategies that enable, facilitate, and acknowledge ecological change.[64] Restoration efforts must be future-proofed against projected sea level rise, allowing for flexibility and redesign of marine and coastal ecosystems. Developing high-quality marine and coastal mapping combined with restoration suitability and predictive models to identify optimal locations for multiple habitats under future climate scenarios should be a priority. Restoration actions to restore biodiversity need to be adopted and aligned with climate science modeling approaches[65] to maximize the resilience and efficacy of restoration.

Other innovative approaches include using genetic technologies to proactively match the adaptability of target species to projected future environments and may increasingly rely on new synthetic biology tools.[66] Conservation efforts should not only focus on mitigating climate change impacts but also on proactively managing emerging opportunities.[67] This involves the inclusion of species and biodiversity beyond national borders, embracing successful and ecologically functioning invasive species where they are established and dominant, and considering where we might need marine species and habitats to be functional in the future.[68] As an example, the Reef Restoration and Adaptation Program (RRAP) in Australia's Great Barrier Reef exemplifies this approach, where integrated climate adaptation into restoration efforts is proliferating.

Marine species are increasingly extending their geographical ranges beyond their native areas in response to climate change and shifts in abiotic conditions.[69] However, species shifts are not always fast enough to respond to rapidly changing environments and may, in some instances, benefit from human intervention to facilitate range expansions. Examples of where such assisted migration might be considered are the spread of the subtropical seagrass *Cymodocea nodosa* northwards in Europe[70] or the deliberate movement of corals further south on the Australian east and west coasts.[71] However, assisted migration needs to be conducted to align with changing temperatures and/or conditions, rather than relying on water movements or other vectors to facilitate colonization. We must consider the range shifts required by these species to support the long-term functioning of marine and coastal ecosystems, which necessitates licensing methods to facilitate this. Alongside such assistance, we also need to consider which phenotypes and genotypes may enhance population resilience and how these are identified and then moved. Emerging tools such as Reef Adapt match optimal donor material for restoration on any particular site based on genetic, biophysical, and climate prediction data.[72] Evidence from the US and the Netherlands indicates that such assisted migration is beginning to commence for seagrass and corals (Unsworth and Govers, unpublished data).

While assisted migration and assisted gene flow are increasingly being considered in terrestrial environments,[73,74] they are currently not on the agenda of many marine management agencies. The authors' experience is that many management agencies are, in fact, opposed to such a movement due to hesitations around the science, which led to an informal approach. Legislative restrictions on such assisted migration are due to the potential impact on the genetic population as an element of biodiversity. Species movements that facilitate gene flow or

Box 3. Coral restoration in the Philippines

The Philippines has a relatively high number of coral restoration projects, supported by its exceptional marine biodiversity and strong interest from external funders. These projects generally focus on rehabilitating degraded reefs and strengthening fisheries management, while those led by the tourism sector can also supplement community livelihoods. Despite this potential, implementation is often constrained by a slow, centralized, and confusing permitting system that requires approvals from multiple agencies. Many practitioners are unaware of the complex requirements, which has led to delays, cancellations, or reliance on local permits alone.[27] Currently, seventeen policies relate to coral restoration, three of which address restoration techniques. These are inconsistent: one requires national permits, another requires local permits, and a third only provides technical guidance. The lack of integration, overlapping jurisdictions, inconsistent definitions, and additional local rules (such as those for MPAs) create a fragmented and confusing regulatory environment. Limited technical expertise within regulatory agencies, particularly at local levels, further exacerbates the situation.[27] Navigating these overlapping permitting requirements is slow and costly, often delaying projects beyond critical windows. Weak enforcement and monitoring reduce incentives to comply, and insufficient oversight allows poorly designed projects to proceed, risking ecological harm. Overall, the existing policy framework fosters inefficiency, abandonment of initiatives, and limited long-term restoration outcomes.

Please cite this article in press as: Unsworth et al., Rethinking marine restoration permitting to urgently advance efforts, Cell Reports Sustainability (2025), https://doi.org/10.1016/j.crsus.2025.100526

Table 1. The use of bionovelty in marine and coastal restoration science at the species and community level creates opportunities to improve current restoration practice

Species-level techniques	Community-level techniques
Assisted gene flow	assisted migration to adjust for climate-driven range expansions
Assisted migration	modeling for sea level rise in site selection
Use of probiotics	restorative aquaculture
Use of established populations of non-native and/or invasive species	manufactured habitats
Selection for climate resilience on population levels	–

migration in the ocean in the context of conservation and restoration have been largely limited to date and are mostly restricted to the relocation of iconic endangered animals, such as the black-footed albatross.[75] However, significant interest is growing in assisted migration, including the development of methods to improve its feasibility and understanding the challenges involved.[76]

All these approaches must consider ecological integrity alongside the well-being, values, and needs of local communities that rely on the ecosystems for the services they provide.[16] Importantly, innovation is at the core of successful restoration. Strategic initiatives, such as the MoonShot (i.e., the US mission to put a human on the moon), succeeded not just because of the funding invested but also because they created a sandbox environment for innovation (through financial, virtual, and actual means of testing and innovating). Achieving marine restoration success necessitates not just the funding that such programs are accumulating, but the willingness of government regulators to facilitate it and create a "marine and coastal restoration sandpit" environment where scientists and practitioners can innovate. However, such innovation comes with an equal or greater level of responsibility, certain ethical considerations, and the need for appropriate risk assessments.[42] This also requires consideration of the associated comments and stakeholders who have the potential to be impacted by a project and can also become major assets to restoration projects.[77,78]

IMPROVED KNOWLEDGE EXCHANGE IS ESSENTIAL

Improved decisions around marine restoration should be grounded in an evidence-based approach. This means necessitating good knowledge exchange of successes, failures, new understanding, and new methods within the restoration community.[14] Given the expanding use of ecological restoration driven by financial instruments, the commercial imperative to plant or create habitat has a strong potential to sidetrack the science in favor of commercial interests (e.g., reduced monitoring, no imperative to share knowledge or understand why something happened or not). Such financial interests may lead to conservation failure, as seen with forest carbon credits.[79]

To avoid "blue-washing" and ensure that marine and coastal restoration follows the science and is evidence-based, the licensing of marine and coastal restoration must become a two-way process that promotes collaboration and understanding between regulators and restoration practitioners. While regulators have many ways to reduce the burden of licensing, the marine and coastal restoration community is also integral to the process. For example, one of the many reasons for hesitation from regulators in licensing marine and coastal restoration is the general sense of skepticism toward such activities and a perception that more research is needed to make decisions—a phenomenon we might call "perfection paralysis."[80] Critics of marine and coastal restoration also refer to it as cosmetic conservation or heroic interference, stating that it provides false hope and is subject to political manipulation, distracting from the real challenge of avoiding catastrophic environmental change.[43,81]

Critics of marine and coastal restoration often dispute the need for restoration. Such critics prefer to point toward alternative recovery pathways or technical solutions, highlighting a lack of significant impact of the restoration or emphasizing the natural recovery capacity of marine ecosystems. Such criticisms are commonly brought about by the problem of shifting baselines[82] resulting from a lack of public reporting of projects and their outcomes.[16] However, we feel that there is a significant disconnect between these criticisms and what is happening in the field (see discussions in Suggett et al.,[11] Braverman,[83] and Hughes et al.[84]). In the same way, there is almost certainly a disconnect between those involved with the decisions on licenses and practitioners (see Boxes 1, 2, and 3 and supplemental information).

To ensure evidence-led marine restoration is undertaken, the wider community needs to share its knowledge openly and make it accessible. Marine and coastal restoration is commonly conducted by a mix of practitioners, scientists, and specialists but may also involve smaller community groups. For example, in Indonesia, policy frameworks for reef restoration have encouraged a variety of practitioners to engage in reef restoration.[85] However, these projects are often not coordinated with broader networks of restoration practitioners or scientists, and only 16% of the identified projects included a post-installation monitoring framework.[85] At every level, projects fail, mistakes are made, but, although success stories do happen, the reporting of the "facts" is often insufficient.[86] There are no public records of where and when such projects occur, and existing records, such as the Society for Ecological Restoration's lists, do not provide clear details of the project's actions or outcomes. Calls have been made to create databases for projects to improve reporting.[86]

A more open environment for licensing must also create a more open environment for sharing knowledge. Regulators need to have transparent processes that not only make licensing easier but also stipulate that all actors, from academics and nongovernmental organizations (NGOs) through to industry, report on their activities.[34] A challenge for achieving such reporting is the presence of incentives to not rigorously report on failures (e.g., due to fears of not obtaining future funding). We are not saying knowledge sharing needs to be done via complex report

Please cite this article in press as: Unsworth et al., Rethinking marine restoration permitting to urgently advance efforts, Cell Reports Sustainability (2025), https://doi.org/10.1016/j.crsus.2025.100526

writing, but, at a minimum, a clear statement of project methods and summary metrics of the project outcomes should be required. Thus, understanding simple key performance indicators to measure success is another area where work needs to be urgently undertaken, translating the complexity of the ecosystems into standardized monitoring and reporting that is simple to measure reliably, repeatedly, and cost-effectively. Funders need to be proactive in ensuring practitioners can conduct such activity.

RESTORATION AT SCALE REQUIRES TIME

Most evidence in marine and coastal restoration indicates that large-scale action both in space and time is key to success. Projects that go big over longer time frames generally succeed, aligning with many of the major terrestrial ecological restoration projects.[14,33] Although this is not always the case, it is as much about overcoming environmental feedback and reaching tipping points[87] as it is about making the right decisions and maximizing the opportunities of resources on a larger scale (e.g., propagules, infrastructure, and finances). Larger resources in bigger projects also allow for a far more holistic view of the restoration to be considered alongside a greater incorporation of social elements alongside the ecological ones.[17,88] This is particularly important to emphasize, as there is increasing evidence of the limited integration of social values into many marine restoration projects.[89]

As marine and coastal restoration is mostly a novel activity, the majority of projects undertaken (seagrass, shellfish, coral reefs, and seaweed) are tiny in size,[33] operating at scales of tens of square meters rather than square kilometers.[33] The notable exception includes some marsh and mangrove projects, which are more advanced in scale with sizes of many tens of thousands of hectares.[7,90] Scaling poses significant issues regarding licensing and capacity, particularly with regard to spanning various coastal land ownership as well as the supply of material and the willingness of regulators to license the supply of donor restoration materials (e.g., seeds, plants, shell cultch, or coral fragments). There is also a significant pinch point regarding projects that require the translocation of restoration materials across borders. Issues of governance that transcend political borders (e.g., the need to transfer restoration materials across borders and associated legal issues) extend to other policy-based issues, such as varying provincial policies and landowner concerns.

Small projects often depend on who has the time and funds to acquire the necessary permissions, where the efforts are disproportionately costly to small projects as the regulatory process is independent of project size. This may result in failed restoration endeavors that otherwise held potential. While such exercises can be excellent learning experiences for actors involved, they do not necessarily solve the overarching need and often miss the initial restoration goal due to delays and misaligned timelines in permitting.

Creating larger projects is part of the solution for marine and coastal restoration, as they can generate economies of scale solutions that spread the costs (and risks) of planning, engagement, and licensing considerations. This does not mean that it must all be done by one major actor, but that areas predefined for restoration offer opportunities for much bigger joined-up thinking. This opens opportunities for a variety of different stakeholders and actors, from community groups to corporate enterprises, to be involved in restoring the marine realm. These efforts need to be part of bigger, more coordinated strategic approaches from governments, which may catalyze major funding opportunities to enable delivery.[15] We should also not fear business if such practices are undertaken with a sustainable focus and a circular economic aspect, which sees profit pushed back into restoration practices.[91] However, although scale helps, the success of restoration projects still depends on how well they are designed and implemented, especially as they are highly complex and require numerous decisions to ensure successful project outcomes.

Marine and coastal restoration at scale is often only achievable through a continuous restoration effort that lasts decades,[92] allowing projects to build on previous success and experience. Ongoing efforts also allow for adaptive management and integration of scientific innovation and refinement of restoration techniques. However, restoration permits are often granted for much shorter periods (e.g., 3–5 years), resulting in a mismatch between long-lasting restoration efforts and permitting that can create several problems. Short permits may cause projects to stop and restart frequently, delaying ecosystem recovery and challenging the achievement of long-term goals. Discontinuity can leave partly restored habitats vulnerable to degradation, reducing the effects of previous restoration work and financial investments. Time and money are spent on repeated permitting instead of restoration work, and securing continuous funding may be difficult if it depends on unpredictable permit renewals. Therefore, alignment of timelines between restoration goals and permitting is crucial for long-lasting restoration projects.

LICENSING AND REGULATION CAN BE AN IMPEDIMENT TO MARINE AND COASTAL RESTORATION

Marine life is highly sensitive to disturbances, exploitation, pollutants, changing environmental conditions, and biological invasions, all of which are stressors linked to human activities, including fisheries, industrial and agricultural activities, global trade, and coastal development.[93] Regulation to control these impacts is indeed an absolute necessity. That said, many would argue that current regulations across many countries are often insufficient in their implementation[94] and/or overly complex, weakening their application.[94] As such, the very regulations aimed at protecting the marine realm can, in some instances, also hinder marine and coastal conservation, especially when restoration is the primary focus. We believe that some regulatory processes actively restrict the capacity of nation-states (see Figure 2) to fulfill their international obligations, facilitated by agreements such as the GBF.

A series of literature case studies from Queensland (AUS), California (US), the UK, and across the Mediterranean clearly sets out the problems of licensing being encountered by marine and coastal restoration projects.[95–97] These studies show that the permitting process is only one part of the problem, and progress is also being hampered by onerous post-approval conditions, including ongoing liability for restorative interventions.[96] Based on our experience of working in marine restoration across

Please cite this article in press as: Unsworth et al., Rethinking marine restoration permitting to urgently advance efforts, Cell Reports Sustainability (2025), https://doi.org/10.1016/j.crsus.2025.100526

CellPress
OPEN ACCESS

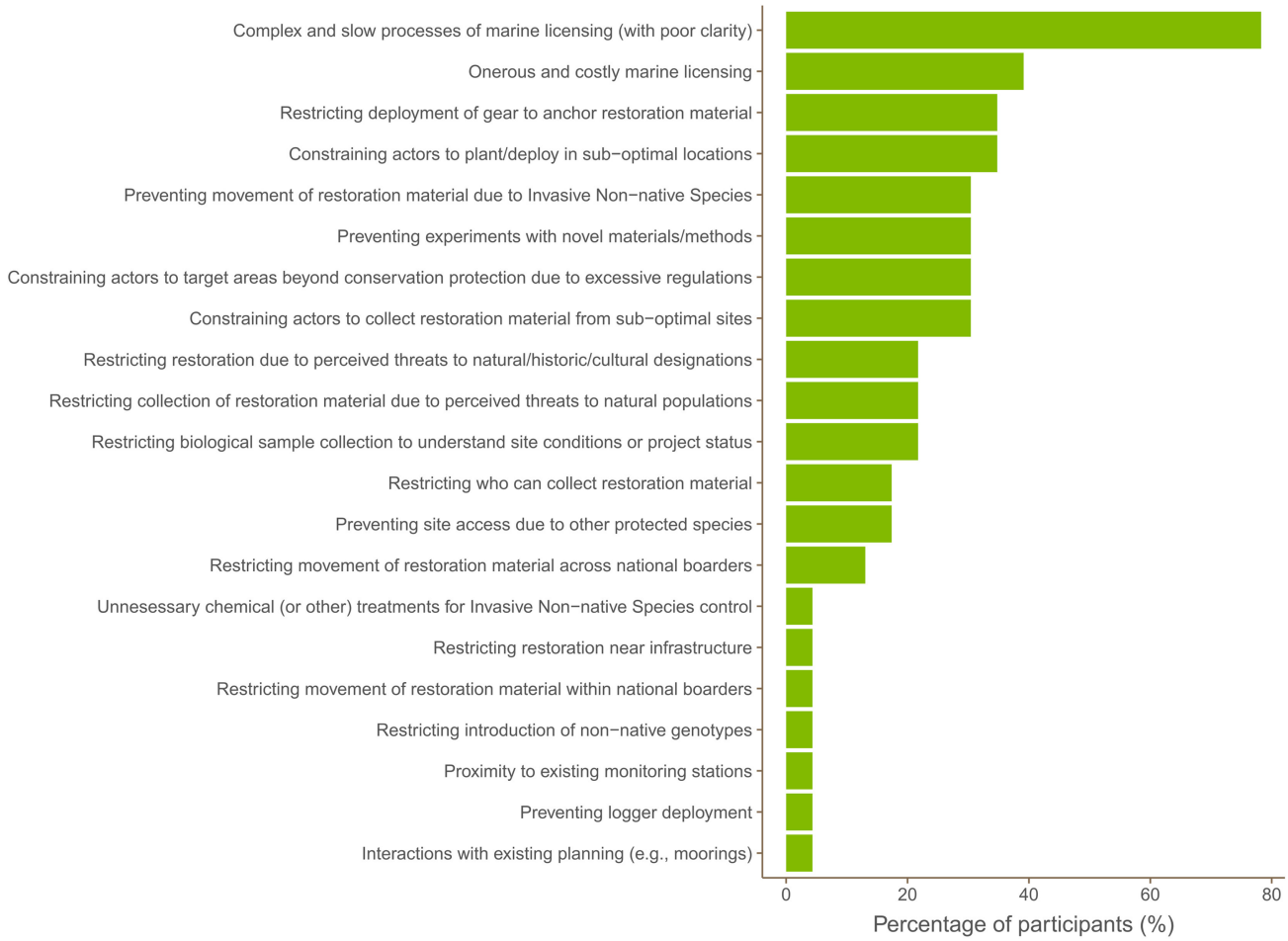

Figure 2. Proportion of the authors who have experienced the following impediments to marine restoration

Data are from 21 scientists (authors) working on marine restoration across 6 ecosystems in 17 countries, all of whom have worked on marine restoration for over 4 years and at least 2 separate major projects. For methods, see supplemental information (N.B. not all of the 25 authors contributed to the survey).

six ecosystems in 18 countries, we observe similar restrictions on these activities to those set out by Bell-James, Foster, and Shumway.[96] We also observe how such restrictions can hinder project implementation, resulting in suboptimal site choices, increased project costs, poor decision-making during the design and implementation of restoration practices, and reduced innovation (see Figure 3).

A consistent problem is often that restoration licensing is very onerous or not possible in marine protected areas (MPAs) due to, for example, protected features or species, even when those are unlikely to be impacted. As a result, this can lead practitioners to choose unprotected or privately owned sites for activities, rather than face the expense and time required for regulatory processes, with the high risk of negative outcomes. In many regions, the only available permits for environmental intervention projects are terrestrial-based and designed to limit habitat destruction; however, they are not fit for purpose for restoration initiatives. We also observe a tendency for some actors to take actions into their own hands, through illegal actions, as has been seen in terrestrial "covert rewilding," to push forward improved outcomes for marine life in response to uncertain regulations and complex licensing procedures.[27]

At the same time, complex licensing procedures likely prevent the facilitation of knowledge sharing, a process that should be encouraged at every opportunity and certainly not curtailed. The absence of robust regulations, or the under-regulation of these activities, on the other hand, can also hinder progress and innovation in marine and coastal restoration, as practitioners have no clear route toward permitting, as is observed in some developing countries.[27] We therefore conclude that existing regulation often restricts restoration potential for success.

Further, climate and biodiversity policies are often developed and implemented by separate institutions and frameworks, leading to missed opportunities for coordinated action. Cross-border collaborative efforts should be emphasized with the aim of creating shared goals and strategies that serve both climate mitigation and biodiversity conservation. Marine and coastal restoration licensing should, therefore, be open to emerging opportunities for climate-proofing marine restoration activities by multiple stakeholders and participants.

Please cite this article in press as: Unsworth et al., Rethinking marine restoration permitting to urgently advance efforts, Cell Reports Sustainability (2025), https://doi.org/10.1016/j.crsus.2025.100526

1. Restoration team spend onerous lengths of time completing licensing paperwork
2. Rogue deployments in response to licensing bottlenecks
3. Restoration restricted next to port infrastructure
4. Presence of protected species prevents site access
5. Restoration material close to deployment site but INNs restricts collection
6. Restoration material cannot be collected as across national and regional borders
7. Challenges understanding site suitability due to licensing of loggers and sample collection
8. Restoration in exposed location as cannot deploy in sheltered MPA
9. Exposure risk of deployment exacerbated by restrictions on deployment gear
10. Restoration material collected in polluted estuary as only place licensed
11. Restrictions on site assessment and monitoring due to time and costs spent on licensing
12. Multiple catchment and coastal threats to habitats remain a limitation to marine restoration

Figure 3. The consequences of restrictions and bottlenecks to restoration in the coastal seascape

A series of suggestions for policy interventions focusing on increased transparency and better integration into coastal policy has been made for Australia[98] and would be applicable internationally. Yet, the uptake of policy interventions appears to be limited. This lack of uptake or acknowledgment of the challenges around licensing is contributing toward missed opportunities and the suspicion that marine restoration projects may often be failing.[99,100] However, in many cases, this failure may even be driven and exacerbated by a need to adhere to unrealistic or inappropriate regulations, or it may be so poorly developed as to include no detailed monitoring and reporting.

LET US BE CLEAR, DEREGULATION IS NOT THE ANSWER

We strongly advocate for an improved licensing system for marine and coastal restoration activities that reflects the international commitments of nations under agreements such as the GBF, which also considers the triple planetary crisis of climate change, biodiversity loss, and pollution. However, we do not support complete deregulation that would facilitate marine and coastal restoration without adequate controls. While acknowledging that there are many and often vast knowledge gaps in our respective fields (or the ocean, as the case may be), we believe that, under strict (but evidence-based) guiding principles, restoration can be conducted without heavy regulation and provide the opportunity to address these knowledge gaps and allow for rapid development of the sector.

There are many examples of cases where uncontrolled or ungoverned restoration practices have led to unintended consequences—for example, in the Philippines, the need to achieve ambitious mangrove planting area targets led to planting on and the destruction of neighboring tidal flats.[101] In other cases, overcollection of restoration materials (such as seagrass seeds) has raised concerns due to the lack of monitoring and reporting on the status of donor populations. The principles of marine restoration are outlined for multiple key habitats[16,40,102,103] and provide strong guidance on the appropriate approaches required. Hence, we advocate for licensing that is evidence-based and enables participants to sign up to those principles without onerous costs and demands.

A NEED FOR EQUITY AND RESPONSIBILITY IN RESTORATION

The urgent need for improved and expanded marine and coastal restoration necessitates rapid decision-making about new programs and projects. While the general expectation around restoration is a net benefit to nearby human populations, this might not always be the case. Forest restoration, for example, has led to loss of access and resource rights in some cases.[77,78] Equity in marine restoration refers to ensuring fairness and justice in the distribution of conservation benefits and burdens, as well as in the participation of different groups in decision-making. The Kunming-Montreal GBF emphasizes human rights, including the rights of Indigenous peoples, local communities, women

Please cite this article in press as: Unsworth et al., Rethinking marine restoration permitting to urgently advance efforts, Cell Reports Sustainability (2025), https://doi.org/10.1016/j.crsus.2025.100526

CellPress
OPEN ACCESS

Figure 4. Six key improvements required to improve licensing and science for marine restoration

and girls, youth, and environmental defenders.[104] It is essential that marine restoration incorporates this perspective.

Ecosystem restoration is most commonly driven by biodiversity and climate change challenges, often disregarding associated yet complex social, cultural, political, economic, institutional, and behavioral aspects.[105] Although we advocate for a cultural shift in how restoration is regulated and licensed, particularly in the context of improving climate change adaptation, we also emphasize that this happens in an equitable manner. Urgency to act is not an excuse for a lack of community engagement and consideration. We also recognize the growing body of evidence that highlights how improved social considerations in ecological restoration improve project outcomes.[106]

THE LAST WORD—AN AGENDA FOR CHANGE

Oceans are experiencing profound and rapid change for the worse, and many of the global marine and coastal conservation efforts amount to little less than a drop in said ocean. For the restoration of marine ecosystems to happen at any genuine, meaningful scale, we believe that an urgent and major cultural shift is required in how licensing and regulation of marine restoration activities are done. There is great promise in restoration or regeneration, but its potential is being held back by unrealistic ecological baselines, outdated priority setting, and increasingly naive views of the rapidity with which the planet is changing. A cultural shift in licensing needs to consider restoration not just from the perspective of recreating habitats but also from ensuring resilient coastal functions and, at the same time, creating stepping-stones, islands, and corridors for future colonization.

We need to think way beyond what we see as baselines (historical or even current) and view a changing climate as a means of rethinking coastal seascapes to better support our future. This requires a licensing system that is robust yet flexible, ensuring it remains fit for purpose and incorporates future thinking and technology in a rapidly changing world. In conclusion to our analysis, we propose six improvements to marine and coastal restoration science and licensing to serve as a catalyst for change (Figure 4).

(1) Proactively embrace opportunities in restoration science to harness novel approaches and techniques (e.g.,

non-native species, assisted gene flow and migration, and genetic technologies) to future-proof for climate change and shift away from historical ecological baselines.

(2) Establish innovation "sandpits" that provide a safe and easily licensed space to develop, test, and refine innovative solutions to improve marine restoration science for all. These may be broad habitat-based networks and/or site-specific sandpits for multi-habitat restoration.

(3) Strategically create marine and coastal restoration areas (potentially even within existing MPAs or National Parks) where ubiquitous permissions and licenses for restoration are provided, subject to practitioners' following specified regulations. Information on these areas and activities should then be shared with other agencies using the marine space to ensure that areas undergoing restoration are, when possible, protected against future disturbances. As with all restoration activities, we argue that the rollout of these initiatives should be guided by the principles of free, prior, and informed consent (FPIC) with local communities and, where possible, conducted in collaboration with such communities.

(4) Establish strong mechanisms and accountability for transparent restoration reporting so that knowledge is shared directly. This is needed, as advancements in restoration science can only be made through an iterative process. This would enable a "learning from failure system" and ensure education across a diverse range of stakeholders.

(5) Create licensing regimes that are (1) streamlined to reduce the need for multiple permissions, (2) cover ecologically realistic time frames to promote developing restoration projects at scale, and (3) are based on the presumption that restoration and habitat creation are positive activities.

(6) Cease charging licensing fees for marine restoration practices and prevent seabed owners from charging fees (while respecting traditional and Indigenous rights) for undertaking marine and coastal restoration. Instead of a fee-based system, an incentivizing system for seabed owners to voluntarily increase the restoration footprint on their land.

DECLARATION OF INTERESTS

The authors declare no competing interests.

SUPPLEMENTAL INFORMATION

Supplemental information can be found online at https://doi.org/10.1016/j.crsus.2025.100526.

REFERENCES

1. Deutsch, C., Penn, J.L., and Lucey, N. (2024). Climate, Oxygen, and the Future of Marine Biodiversity. Annu. Rev. Mar. Sci. *16*, 217–245. https://doi.org/10.1146/annurev-marine-040323-095231.

2. Dietzel, A., Bode, M., Connolly, S.R., and Hughes, T.P. (2021). The population sizes and global extinction risk of reef-building coral species at biogeographic scales. Nat. Ecol. Evol. *5*, 663–669. https://doi.org/10.1038/s41559-021-01393-4.

3. Braun, C.D., Lezama-Ochoa, N., Farchadi, N., Arostegui, M.C., Alexander, M., Allyn, A., Bograd, S.J., Brodie, S., Crear, D.P., Curtis, T.H., et al. (2023). Widespread habitat loss and redistribution of marine top predators in a changing ocean. Sci. Adv. *9*, eadi2718. https://doi.org/10.1126/sciadv.adi2718.

4. Dunic, J.C., Brown, C.J., Connolly, R.M., Turschwell, M.P., and Côté, I. M. (2021). Long-term declines and recovery of meadow area across the world's seagrass bioregions. Glob. Change Biol. *27*, 4096–4109. https://doi.org/10.1111/gcb.15684.

5. Goldberg, L., Lagomasino, D., Thomas, N., and Fatoyinbo, T. (2020). Global declines in human-driven mangrove loss. Glob. Change Biol. *26*, 5844–5855. https://doi.org/10.1111/gcb.15275.

6. McKinley, E., Pagès, J.F., Alexander, M., Burdon, D., and Martino, S. (2020). Uses and management of saltmarshes: A global survey. Estuarine Coastal Shelf Sci. *243*, 106840. https://doi.org/10.1016/j.ecss.2020.106840.

7. Duarte, C.M., Agusti, S., Barbier, E., Britten, G.L., Castilla, J.C., Gattuso, J.-P., Fulweiler, R.W., Hughes, T.P., Knowlton, N., Lovelock, C.E., et al. (2020). Rebuilding marine life. Nature *580*, 39–51. https://doi.org/10.1038/s41586-020-2146-7.

8. Waltham, N.J., Elliott, M., Lee, S.Y., Lovelock, C., Duarte, C.M., Buelow, C., Simenstad, C., Nagelkerken, I., Claassens, L., Wen, C.K.-C., et al. (2020). UN Decade on Ecosystem Restoration 2021–2030—What Chance for Success in Restoring Coastal Ecosystems? Front. Mar. Sci. *7*, 71.

9. Fu, C., Steckbauer, A., Mann, H., and Duarte, C.M. (2024). Achieving the Kunming–Montreal global biodiversity targets for blue carbon ecosystems. Nat. Rev. Earth Environ. *5*, 538–552. https://doi.org/10.1038/s43017-024-00566-6.

10. Perissi, I. (2025). Assessing the EU27 Potential to Meet the Nature Restoration Law Targets. Environ. Manag. *75*, 711–729. https://doi.org/10.1007/s00267-024-02107-9.

11. Suggett, D.J., Guest, J., Camp, E.F., Edwards, A., Goergen, L., Hein, M., Humanes, A., Levy, J.S., Montoya-Maya, P.H., Smith, D.J., et al. (2024). Restoration as a meaningful aid to ecological recovery of coral reefs. npj Ocean Sustain. *3*, 20. https://doi.org/10.1038/s44183-024-00056-8.

12. van Oppen, M.J.H., Gates, R.D., Blackall, L.L., Cantin, N., Chakravarti, L. J., Chan, W.Y., Cormick, C., Crean, A., Damjanovic, K., Epstein, H., et al. (2017). Shifting paradigms in restoration of the world's coral reefs. Glob. Change Biol. *23*, 3437–3448. https://doi.org/10.1111/gcb.13647.

13. Su, J., Friess, D.A., and Gasparatos, A. (2021). A meta-analysis of the ecological and economic outcomes of mangrove restoration. Nat. Commun. *12*, 5050. https://doi.org/10.1038/s41467-021-25349-1.

14. Saunders, M.I., Doropoulos, C., Bayraktarov, E., Babcock, R.C., Gorman, D., Eger, A.M., Vozzo, M.L., Gillies, C.L., Vanderklift, M.A., Steven, A.D.L., et al. (2020). Bright Spots in Coastal Marine Ecosystem Restoration. Curr. Biol. *30*, R1500–R1510. https://doi.org/10.1016/j.cub.2020.10.056.

15. Stewart-Sinclair, P.J., Purandare, J., Bayraktarov, E., Waltham, N., Reeves, S., Statton, J., Sinclair, E.A., Brown, B.M., Shribman, Z.I., and Lovelock, C.E. (2020). Blue Restoration – Building Confidence and Overcoming Barriers. Front. Mar. Sci. *7*, 541700. https://doi.org/10.3389/fmars.2020.541700.

16. Unsworth, R.K.F., Jones, B.L.H., Bertelli, C.M., Coals, L., Cullen-Unsworth, L.C., Mendzil, A.F., Rees, S.C., Taylor, F., Walter, B., and Evans, A.J. (2025). Ten golden rules for restoration to secure resilient and just seagrass social-ecological systems. Plants People Planet *7*, 33–48. https://doi.org/10.1002/ppp3.10560.

17. Suding, K., Higgs, E., Palmer, M., Callicott, J.B., Anderson, C.B., Baker, M., Gutrich, J.J., Hondula, K.L., LaFevor, M.C., Larson, B.M.H., et al.

(2015). Conservation. Committing to ecological restoration. Science *348*, 638–640. https://doi.org/10.1126/science.aaa4216.

18. Bilawal Khaskheli, M., Wang, S., Zhang, X., Shamsi, I.H., Shen, C., Rasheed, S., Ibrahim, Z., and Baloch, D.M. (2023). Technology advancement and international law in marine policy, challenges, solutions and future prospective. Front. Mar. Sci. *10*, 1258924. https://doi.org/10.3389/fmars.2023.1258924.
19. Evans, A.J., Ford, E., and Cullen-Unsworth, L. (2025). Connecting governance and practice views on the barriers and solutions to scaled seagrass restoration in the UK. Mar. Policy *180*, 106781. https://doi.org/10.1016/j.marpol.2025.106781.
20. Vergés, A., Campbell, A.H., Wood, G., Kajlich, L., Eger, A.M., Cruz, D., Langley, M., Bolton, D., Coleman, M.A., Turpin, J., et al. (2020). Operation Crayweed: Ecological and sociocultural aspects of restoring Sydney's underwater forests. Eco. Management Restoration *21*, 74–85. https://doi.org/10.1111/emr.12413.
21. Babcock, R.C., Kelly, S., Shears, N.T., Walker, J.W., and Willis, T.J. (1999). Changes in community structure in temperate marine reserves. Mar. Ecol. Prog. Ser. *189*, 125–134. https://doi.org/10.3354/meps189125.
22. Kumagai, J.A., Goodman, M.C., Villaseñor-Derbez, J.C., Schoeman, D. S., Cavanuagh, K.C., Bell, T.W., Micheli, F., De Leo, G., and Arafeh-Dalmau, N. (2024). Marine Protected Areas That Preserve Trophic Cascades Promote Resilience of Kelp Forests to Marine Heatwaves. Glob. Change Biol. *30*, e17620. https://doi.org/10.1111/gcb.17620.
23. Turnbull, J.W., Shah Esmaeili, Y., Clark, G.F., Figueira, W.F., Johnston, E. L., and Ferrari, R. (2018). Key drivers of effectiveness in small marine protected areas. Biodivers. Conserv. *27*, 2217–2242. https://doi.org/10.1007/s10531-018-1532-z.
24. Nowakowski, A.J., Canty, S.W.J., Bennett, N.J., Cox, C.E., Valdivia, A., Deichmann, J.L., Akre, T.S., Bonilla-Anariba, S.E., Costedoat, S., and McField, M. (2023). Co-benefits of marine protected areas for nature and people. Nat. Sustain. *6*, 1210–1218. https://doi.org/10.1038/s41893-023-01150-4.
25. Guarnieri, G., Bevilacqua, S., Figueras, N., Tamburello, L., and Fraschetti, S. (2020). Large-Scale Sea Urchin Culling Drives the Reduction of Subtidal Barren Grounds in the Mediterranean Sea. Front. Mar. Sci. *7*, 514009. https://doi.org/10.3389/fmars.2020.00519.
26. Bursic, J., Layton, C., Carnell, P., Pocklington, J.B., Breschkin, S., and Francis, P. (2025). Cultivation Handbook for Ecklonia radiata: Port Phillip Bay. 978-0-7300-0425-7.
27. Matorres, D.E., Fabinyi, M., Horigue, V., Novilla, C.T., and Baria-Rodriguez, M.V. (2024). Institutional dimensions of coral reef restoration in the Philippines. Environ. Sci. Policy *156*, 103734. https://doi.org/10.1016/j.envsci.2024.103734.
28. Eger, A.M., Marzinelli, E.M., Beas-Luna, R., Blain, C.O., Blamey, L.K., Byrnes, J.E.K., Carnell, P.E., Choi, C.G., Hessing-Lewis, M., Kim, K.Y., et al. (2023). The value of ecosystem services in global marine kelp forests. Nat. Commun. *14*, 1894. https://doi.org/10.1038/s41467-023-37385-0.
29. Fonseca, M.S. (2011). Addy Revisited: What has changed with seagrass restoration in 64 years? Ecol. Restor. *29*, 73–81. https://doi.org/10.3368/er.29.1-2.73.
30. Esteves, L.S. (2013). Is managed realignment a sustainable long-term coastal management approach? J. Coastal Res. *65*, 933–938. https://doi.org/10.2112/SI65-158.1.
31. Lovelock, C.E., Barbier, E., and Duarte, C.M. (2022). Tackling the mangrove restoration challenge. PLoS Biol. *20*, e3001836. https://doi.org/10.1371/journal.pbio.3001836.
32. Simon, D., Kuhlmann, S., Stamm, J., Canzler, W., Owen, R., and Pansera, M. (2019). Handbook on Science and Public Policy (Edward Elgar Publishing).
33. van Katwijk, M.M., Thorhaug, A., Marbà, N., Orth, R.J., Duarte, C.M., Kendrick, G.A., Althuizen, I.H.J., Balestri, E., Bernard, G., Cambridge, M.L., et al. (2016). Global analysis of seagrass restoration: the importance of large-scale planting. J. Appl. Ecol. *53*, 567–578. https://doi.org/10.1111/1365-2664.12562.
34. Gatt, Y.M., Walton, R.W., Andradi-Brown, D.A., Spalding, M.D., Acosta-Velázquez, J., Adame, M.F., Barros, F., Beeston, M.A., Bernardino, A.F., Buelow, C.A., et al. (2024). The Mangrove Restoration Tracker Tool: Meeting local practitioner needs and tracking progress toward global targets. One Earth *7*, 2072–2085. https://doi.org/10.1016/j.oneear.2024.09.004.
35. Unsworth, R.K.F., and Rees, S.C. (2025). The road to seagrass restoration at scale using engineering. Ecol. Eng. *215*, 107607.
36. Purandare, J., de Sousa de Saboya, R., Bayraktarov, E., Boström-Einarsson, L., Carnell, P.E., Eger, A.M., Le Port, A., Macreadie, P.I., Reeves, S. E., van Kampen, P., et al. (2024). Database for marine and coastal restoration projects in Australia and New Zealand. Eco. Management Restoration *25*, 14–20. https://doi.org/10.1111/emr.12596.
37. Sweet, M., Burian, A., and Bulling, M. (2021). Corals as canaries in the coalmine: Towards the incorporation of marine ecosystems into the 'One Health' concept. J. Invertebr. Pathol. *186*, 107538. https://doi.org/10.1016/j.jip.2021.107538.
38. van Vuuren, D.P., Doelman, J.C., Schmidt Tagomori, I., Beusen, A.H.W., Cornell, S.E., Röckstrom, J., Schipper, A.M., Stehfest, E., Ambrosio, G., van den Berg, M., et al. (2025). Exploring pathways for world development within planetary boundaries. Nature *641*, 910–916. https://doi.org/10.1038/s41586-025-08928-w.
39. Peixoto, R.S., Voolstra, C.R., Sweet, M., Duarte, C.M., Carvalho, S., Villela, H., Lunshof, J.E., Gram, L., Woodhams, D.C., Walter, J., et al. (2022). Harnessing the microbiome to prevent global biodiversity loss. Nat. Microbiol. *7*, 1726–1735. https://doi.org/10.1038/s41564-022-01173-1.
40. Quigley, K.M., Hein, M., and Suggett, D.J. (2022). Translating the 10 golden rules of reforestation for coral reef restoration. Conserv. Biol. *36*, e13890. https://doi.org/10.1111/cobi.13890.
41. Higgs, E.S., Harris, J.A., Heger, T., Hobbs, R.J., Murphy, S.D., and Suding, K.N. (2018). Keep ecological restoration open and flexible. Nat. Ecol. Evol. *2*, 580. https://doi.org/10.1038/s41559-018-0483-9.
42. Volpe, J.P., Higgs, E.S., Jeschke, J.M., Barnhill, K., Brunk, C., Dudney, J., Govers, L.L., Hobbs, R.J., Keenleyside, K., Murphy, S.D., et al. (2024). Bionovelty and ecological restoration. Restor. Ecol. *32*, e14152. https://doi.org/10.1111/rec.14152.
43. Streit, R.P., Morrison, T.H., and Bellwood, D.R. (2024). Coral reefs deserve evidence-based management not heroic interference. Nat. Clim. Change *14*, 773–775. https://doi.org/10.1038/s41558-024-02063-6.
44. Lennon, M. (2017). Moral-Material Ontologies of Nature Conservation: Exploring the Discord between Ecological Restoration and Novel Ecosystems. Environ. Values *26*, 5–29. https://doi.org/10.3197/096327117X14809634978474.
45. De Poorter, M., Darby, C., and MacKay, J. (2009). Marine Menace: Alien Invasive Species in the Marine Environment (International Union for Conservation of Nature and Natural Resources), p. 30.
46. Giakoumi, S., Katsanevakis, S., Albano, P.G., Azzurro, E., Cardoso, A.C., Cebrian, E., Deidun, A., Edelist, D., Francour, P., Jimenez, C., et al. (2019). Management priorities for marine invasive species. Sci. Total Environ. *688*, 976–982. https://doi.org/10.1016/j.scitotenv.2019.06.282.
47. Ren, H., Lu, H., Shen, W., Huang, C., Guo, Q., Li, Z., and Jian, S. (2009). Sonneratia apetala Buch.Ham. in the mangrove ecosystems of China: An invasive species or restoration species? Ecol. Eng. *35*, 1243–1248. https://doi.org/10.1016/j.ecoleng.2009.05.008.
48. Ainouche, M., and Gray, A. (2016). Invasive Spartina: lessons and challenges. Biol. Invas. *18*, 2119–2122. https://doi.org/10.1007/s10530-016-1201-7.

49. Hobbs, R.J., Higgs, E., and Harris, J.A. (2009). Novel ecosystems: implications for conservation and restoration. Trends Ecol. Evol. *24*, 599–605. https://doi.org/10.1016/j.tree.2009.05.012.

50. Thieltges, D., Strasser, M., and Reise, K. (2003). The American slipper limpet Crepidula fornicata (L.) in the northern Wadden Sea 70 years after its introduction. Helgol. Mar. Res. *57*, 27–33. https://doi.org/10.1007/s10152-002-0119-x.

51. Thomsen, M.S., Wernberg, T., Stæhr, P.A., and Pedersen, M.F. (2006). Spatio-temporal distribution patterns of the invasive macroalga Sargassum muticum within a Danish Sargassum-bed. Helgol. Mar. Res. *60*, 50–58. https://doi.org/10.1007/s10152-005-0016-1.

52. Christianen, M.J.A., Lengkeek, W., Bergsma, J.H., Coolen, J.W.P., Didderen, K., Dorenbosch, M., Driessen, F.M.F., Kamermans, P., Reuchlin-Hugenholtz, E., Sas, H., et al. (2018). Return of the native facilitated by the invasive? Population composition, substrate preferences and epibenthic species richness of a recently discovered shellfish reef with native European flat oysters (Ostrea edulis) in the North Sea. Mar. Biol. Res. *14*, 590–597. https://doi.org/10.1080/17451000.2018.1498520.

53. Zimmer, M. (2018). Ecosystem Design: When Mangrove Ecology Meets Human Needs. In Threats to Mangrove Forests: Hazards, Vulnerability, and Management, C. Makowski and C.W. Finkl, eds. (Springer International Publishing), pp. 367–376. https://doi.org/10.1007/978-3-319-73016-5_16.

54. Vozzo, M.L., Buelow, C.A., Sievers, M., Adame, M.F., Branson, P., Brown, M., Crosswell, J.R., Doropoulos, C., Gilby, B.L., Martinez-Baena, F., et al. (2024). Achieving at-scale seascape restoration by optimising cross-habitat facilitative processes. npj Ocean Sustain. *3*, 57. https://doi.org/10.1038/s44183-024-00095-1.

55. Muehlbauer, F., Fraser, D., Brenner, M., Van Nieuwenhove, K., Buck, B. H., Strand, O., Mazurié, J., Thorarinsdottir, G., Dolmer, P., O'Beirn, F., et al. (2014). Bivalve aquaculture transfers in Atlantic Europe. Part A: Transfer activities and legal framework. Ocean & Coastal Management *89*, 127–138. https://doi.org/10.1016/j.ocecoaman.2013.12.003.

56. McAfee, D., and Connell, S.D. (2021). The global fall and rise of oyster reefs. Front. Ecol. Environ. *19*, 118–125. https://doi.org/10.1002/fee.2291.

57. Gerritsen, H. (2005). What happened in 1953? The Big Flood in the Netherlands in retrospect. Philos. Trans. A Math. Phys. Eng. Sci. *363*, 1271–1291. https://doi.org/10.1098/rsta.2005.1568.

58. Yeung, Y.-m. (2001). Coastal mega-cities in Asia: transformation, sustainability and management. Ocean & Coastal Management *44*, 319–333. https://doi.org/10.1016/S0964-5691(01)00053-9.

59. Luo, J., Sun, Z., Lu, L., Xiong, Z., Cui, L., and Mao, Z. (2022). Rapid expansion of coastal aquaculture ponds in Southeast Asia: Patterns, drivers and impacts. J. Environ. Manag. *315*, 115100. https://doi.org/10.1016/j.jenvman.2022.115100.

60. Pörtner, H.O., Roberts, D.C., Masson-Delmotte, V., Zhai, P., Tignor, M., and Poloczanska, E. (2019). IPCC Special Report on the Ocean and Cryosphere in a Changing Climate (International Panel on Climate Change, United Nations).

61. Scheffers, B.R., De Meester, L., Bridge, T.C.L., Hoffmann, A.A., Pandolfi, J.M., Corlett, R.T., Butchart, S.H.M., Pearce-Kelly, P., Kovacs, K.M., Dudgeon, D., et al. (2016). The broad footprint of climate change from genes to biomes to people. Science *354*, aaf7671. https://doi.org/10.1126/science.aaf7671.

62. McCormack, P.C. (2019). Reforming restoration law to support climate change adaptation. In Ecological Restoration Law, A. Akhtar-Khavari and B.J. Richardson, eds. (Routledge), pp. 265–287. https://doi.org/10.4324/9780429468315-12.

63. Wood, G., Marzinelli, E.M., Coleman, M.A., Campbell, A.H., Santini, N.S., Kajlich, L., Verdura, J., Wodak, J., Steinberg, P.D., and Vergés, A. (2019). Restoring subtidal marine macrophytes in the Anthropocene: trajectories and future-proofing. Mar. Freshw. Res. *70*, 936–951. https://doi.org/10.1071/MF18226.

64. Moore, J.W., and Schindler, D.E. (2022). Getting ahead of climate change for ecological adaptation and resilience. Science *376*, 1421–1426. https://doi.org/10.1126/science.abo3608.

65. Cabral, J.S., Mendoza-Ponce, A., da Silva, A.P., Oberpriller, J., Mimet, A., Kieslinger, J., Berger, T., Blechschmidt, J., Brönner, M., Classen, A., et al. (2024). The road to integrate climate change projections with regional land-use–biodiversity models. People Nat. *6*, 1716–1741. https://doi.org/10.1002/pan3.10472.

66. Coleman, M.A., Wood, G., Filbee-Dexter, K., Minne, A.J.P., Goold, H.D., Vergés, A., Marzinelli, E.M., Steinberg, P.D., and Wernberg, T. (2020). Restore or Redefine: Future Trajectories for Restoration. Front. Mar. Sci. *7*, 237. https://doi.org/10.3389/fmars.2020.00237.

67. Syahid, L.N., Sakti, A.D., Ward, R., Rosleine, D., Windupranata, W., and Wikantika, K. (2023). Optimizing the spatial distribution of Southeast Asia mangrove restoration based on zonation, species and carbon projection schemes. Estuarine Coastal Shelf Sci. *293*, 108477. https://doi.org/10.1016/j.ecss.2023.108477.

68. Gormley, K.S.G., Hull, A.D., Porter, J.S., Bell, M.C., and Sanderson, W.G. (2015). Adaptive management, international co-operation and planning for marine conservation hotspots in a changing climate. Mar. Policy *53*, 54–66. https://doi.org/10.1016/j.marpol.2014.11.017.

69. Wesselmann, M., Hendriks, I.E., Johnson, M., Jordà, G., Mineur, F., and Marbà, N. (2024). Increasing spread rates of tropical non-native macrophytes in the Mediterranean Sea. Glob. Change Biol. *30*, e17249. https://doi.org/10.1111/gcb.17249.

70. Duarte, B., Martins, I., Rosa, R., Matos, A.R., Roleda, M.Y., Reusch, T.B. H., Engelen, A.H., Serrão, E.A., Pearson, G.A., Marques, J.C., et al. (2018). Climate Change Impacts on Seagrass Meadows and Macroalgal Forests: An Integrative Perspective on Acclimation and Adaptation Potential. Front. Mar. Sci. *5*, 190. https://doi.org/10.3389/fmars.2018.00190.

71. Beger, M., Sommer, B., Harrison, P.L., Smith, S.D.A., and Pandolfi, J.M. (2014). Conserving potential coral reef refuges at high latitudes. Divers. Distrib. *20*, 245–257. https://doi.org/10.1111/ddi.12140.

72. Wood, G.V., Griffin, K.J., van der Mheen, M., Breed, M.F., Edgeloe, J.M., Grimaldi, C., Minne, A.J.P., Popovic, I., Filbee-Dexter, K., van Oppen, M. J.H., Wernberg, T., and Coleman, M.A. (2024). Reef Adapt: A tool to inform climate-smart marine restoration and management decisions. Communications Biology *7*, 1368. https://doi.org/10.1038/s42003-024-06970-4.

73. Seddon, P., and Redford, K. (2025). Current and future challenges to conservation translocations. Nat. Rev. Biodivers. *1*, 197–208. https://doi.org/10.1038/s44358-025-00020-5.

74. Godefroid, S., Lacquaye, S., Ensslin, A., Dalrymple, S., Abeli, T., Branwood, H., Ferrando Pardo, I., Ferrer Gallego, P.P., Zippel, E., Gouveia, L., et al. (2025). Current state of plant conservation translocations across Europe: motivations, challenges and outcomes. Biodivers. Conserv. *34*, 769–792. https://doi.org/10.1007/s10531-025-03013-0.

75. Soorae, P.S. (2018). Global Reintroduction Perspectives. Case studies from around the globe. IUCN/SSC Reintroduction Specialist Group, Gland, Switzerland and Environment Agency, Abu Dhabi, United AE.

76. Gibbs, M.T., Gibbs, B.L., Newlands, M., and Ivey, J. (2021). Scaling up the global reef restoration activity: Avoiding ecological imperialism and ongoing colonialism. PLoS One *16*, e0250870. https://doi.org/10.1371/journal.pone.0250870.

77. Kandel, M., Agaba, G., Alare, R.S., Addoah, T., and Schreckenberg, K. (2021). Assessing Social Equity in Farmer-Managed Natural Regeneration (FMNR) Interventions: Findings from Ghana. Ecol. Restor. *39*, 64–76. https://doi.org/10.3368/er.39.1-2.64.

78. Hajjar, R., Oldekop, J.A., Cronkleton, P., Newton, P., Russell, A.J.M., and Zhou, W. (2021). A global analysis of the social and environmental outcomes of community forests. Nat. Sustain. *4*, 216–224. https://doi.org/10.1038/s41893-020-00633-y.

79. Jones, J.P.G., and Lewis, S.L. (2023). Forest carbon offsets are failing. Science *381*, 830–831. https://doi.org/10.1126/science.adj6951.

80. Tan, Y.M., Dalby, O., Kendrick, G.A., Statton, J., Sinclair, E.A., Fraser, M. W., Macreadie, P.I., Gillies, C.L., Coleman, R.A., Waycott, M., et al. (2020). Seagrass Restoration Is Possible: Insights and Lessons From Australia and New Zealand. Front. Mar. Sci. *7*. https://doi.org/10.3389/fmars.2020.00617.

81. McAfee, D., Costanza, R., and Connell, S.D. (2021). Valuing marine restoration beyond the 'too small and too expensive'. Trends Ecol. Evol. *36*, 968–971. https://doi.org/10.1016/j.tree.2021.08.002.

82. Guerrero-Gatica, M., Aliste, E., and Simonetti, J.A. (2019). Shifting Gears for the Use of the Shifting Baseline Syndrome in Ecological Restoration. Sustainability *11*, 1131–1144. https://doi.org/10.3390/su11051458.

83. Braverman, I. (2016). Biopolarity: Coral Scientists between Hope and Despair. Anthropol. Now *8*, 26–40. https://doi.org/10.1080/19428200.2016.1242908.

84. Hughes, T.P., Baird, A.H., Morrison, T.H., and Torda, G. (2023). Principles for coral reef restoration in the anthropocene. One Earth *6*, 656–665. https://doi.org/10.1016/j.oneear.2023.04.008.

85. Razak, T.B., Boström-Einarsson, L., Alisa, C.A.G., Vida, R.T., and Lamont, T.A.C. (2022). Coral reef restoration in Indonesia: A review of policies and projects. Mar. Policy *137*, 104940. https://doi.org/10.1016/j.marpol.2021.104940.

86. Eger, A.M., Earp, H.S., Friedman, K., Gatt, Y., Hagger, V., Hancock, B., Kaewsrikhaw, R., Mcleod, E., Moore, A.M., Niner, H.J., et al. (2022). The need, opportunities, and challenges for creating a standardized framework for marine restoration monitoring and reporting. Biol. Conserv. *266*, 109429. https://doi.org/10.1016/j.biocon.2021.109429.

87. Maxwell, P.S., Eklöf, J.S., van Katwijk, M.M., O'Brien, K.R., de La Torre-Castro, M., Boström, C., Bouma, T.J., Krause-Jensen, D., Unsworth, R. K.F., van Tussenbroek, B.I., et al. (2017). The fundamental role of ecological feedback mechanisms for the adaptive management of seagrass ecosystems – a review. Biol. Rev. Camb. Philos. Soc. *92*, 1521–1538. https://doi.org/10.1111/brv.12294.

88. Kenny, I., Connell, S.D., Drew, G., Wright, A., Carruthers, S., and McAfee, D. (2023). Aligning social and ecological goals for successful marine restoration. Biol. Conserv. *288*, 110357. https://doi.org/10.1016/j.biocon.2023.110357.

89. Rodríguez-Rodríguez, A., Palacios, M.M., Wartman, M., Costa, D.P., Macreadie, P.I., and Rasheed, A.R. (2025). Current trends and future directions for integrating social values into mangrove restoration. Restor. Ecol. *33*, e70139. https://doi.org/10.1111/rec.70139.

90. Perera, N., Lokupitiya, E., Halwatura, D., and Udagedara, S. (2022). Quantification of blue carbon in tropical salt marshes and their role in climate change mitigation. Sci. Total Environ. *820*, 153313. https://doi.org/10.1016/j.scitotenv.2022.153313.

91. Filbee-Dexter, K., Wernberg, T., Barreiro, R., Coleman, M.A., de Bettignies, T., Feehan, C.J., Franco, J.N., Hasler, B., Louro, I., Norderhaug, K.M., et al. (2022). Leveraging the blue economy to transform marine forest restoration. J. Phycol. *58*, 198–207. https://doi.org/10.1111/jpy.13239.

92. Orth, R.J., Lefcheck, J.S., McGlathery, K.S., Aoki, L., Luckenbach, M.W., Moore, K.A., Oreska, M.P.J., Snyder, R., Wilcox, D.J., and Lusk, B. (2020). Restoration of seagrass habitat leads to rapid recovery of coastal ecosystem services. Sci. Adv. *6*, eabc6434. https://doi.org/10.1126/sciadv.abc6434.

93. Turschwell, M.P., Connolly, R.M., Dunic, J.C., Sievers, M., Buelow, C.A., Pearson, R.M., Tulloch, V.J.D., Côté, I.M., Unsworth, R.K.F., Collier, C.J., et al. (2021). Anthropogenic pressures and life history predict trajectories of seagrass meadow extent at a global scale. Proc. Natl. Acad. Sci. USA *118*, e2110802118. https://doi.org/10.1073/pnas.2110802118.

94. Boyes, S.J., and Elliott, M. (2014). Marine legislation – The ultimate 'horrendogram': International law, European directives & national implementation. Mar. Pollut. Bull. *86*, 39–47. https://doi.org/10.1016/j.marpolbul.2014.06.055.

95. Ponsford, M. (2022). Queen Elizabeth owns most of the U.K. seabed. That's slowing conservation work. National Geographic.

96. Bell-James, J., Foster, R., and Shumway, N. (2023). The permitting process for marine and coastal restoration: A barrier to achieving global restoration targets? Conserv. Sci. Pract. *5*, e13050. https://doi.org/10.1111/csp2.13050.

97. van Tatenhove, J.P.M., Ramírez-Monsalve, P., Carballo-Cárdenas, E., Papadopoulou, N., Smith, C.J., Alferink, L., Ounanian, K., and Long, R. (2021). The governance of marine restoration: insights from three cases in two European seas. Restor. Ecol. *29*, e13288. https://doi.org/10.1111/rec.13288.

98. Shumway, N., Bell-James, J., Fitzsimons, J.A., Foster, R., Gillies, C., and Lovelock, C.E. (2021). Policy solutions to facilitate restoration in coastal marine environments. Mar. Policy *134*, 104789. https://doi.org/10.1016/j.marpol.2021.104789.

99. Boström-Einarsson, L., Babcock, R.C., Bayraktarov, E., Ceccarelli, D., Cook, N., Ferse, S.C.A., Hancock, B., Harrison, P., Hein, M., Shaver, E., et al. (2020). Coral restoration – A systematic review of current methods, successes, failures and future directions. PLoS One *15*, e0226631. https://doi.org/10.1371/journal.pone.0226631.

100. Schmidt-Roach, S., Knorr, T., Roch, C., Klaus, R., Klepac, C., Klein, S.G., and Duarte, C.M. (2025). Cost-efficiency and effectiveness of coral restoration pathways. Restor. Ecol. *33*, e14326. https://doi.org/10.1111/rec.14326.

101. Wodehouse, D.C.J., and Rayment, M.B. (2019). Mangrove area and propagule number planting targets produce sub-optimal rehabilitation and afforestation outcomes. Estuarine Coastal Shelf Sci. *222*, 91–102. https://doi.org/10.1016/j.ecss.2019.04.003.

102. Lewis, R.R., Brown, B.M., and Flynn, L.L. (2019). Chapter 24 - Methods and Criteria for Successful Mangrove Forest Rehabilitation. In Coastal Wetlands, Second Edition, G.M.E. Perillo, E. Wolanski, D.R. Cahoon, and C.S. Hopkinson, eds. (Elsevier), pp. 863–887.

103. Fitzsimons, J.A., Branigan, S., Gillies, C.L., Brumbaugh, R.D., Cheng, J., DeAngelis, B.M., Geselbracht, L., Hancock, B., Jeffs, A., McDonald, T., et al. (2020). Restoring shellfish reefs: Global guidelines for practitioners and scientists. Conserv. Sci. Pract. *2*, e198. https://doi.org/10.1111/csp2.198.

104. Tugendhat, H., Castillo, A.R., Figueroa, V.E., Ngomo, A.K., Corpuz, J., Jonas, H., and Chepkorir, M. (2023). Respecting the rights and leadership of Indigenous Peoples and local communities in realizing global goals. Oryx *57*, 275–276. https://doi.org/10.1017/S0030605323000406.

105. Mansourian, S., Djenontin, I.N.S., Elias, M., Oldekop, J.A., Derkyi, M.A. A., Kull, C.A., and Pacheco, P. (2025). Ecosystem restoration centered in people. Restor. Ecol. *33*, e70049. https://doi.org/10.1111/rec.70049.

106. Löfqvist, S., Kleinschroth, F., Bey, A., de Bremond, A., DeFries, R., Dong, J., Fleischman, F., Lele, S., Martin, D.A., Messerli, P., et al. (2023). How Social Considerations Improve the Equity and Effectiveness of Ecosystem Restoration. Bioscience *73*, 134–148. https://doi.org/10.1093/biosci/biac099.

CRSUS, Volume *2*

Supplemental information

Rethinking marine restoration permitting

to urgently advance efforts

Richard K.F. Unsworth, Michael Sweet, Laura L. Govers, Sophie von der Heyden, Adriana Vergés, Daniel A. Friess, Benjamin L.H. Jones, Margaux A.A. Monfared, Rune C. Steinfurth, Jose M. Fariñas-Franco, Leanne C. Cullen-Unsworth, Timi L. Banke, Fiona Tomas, Bowdoin W. Lusk, Anouska F. Mendzil, Alison J. Debney, William G. Sanderson, Esther Thomsen, Joanne Preston, Elizabeth A. Lacey, Kristina Boerder, Rowana Walton, Tali Vadi, Jen Brand, and Maike Paul

Supplementary information

Supplemental Notes

Supplemental Figures

Figure S19. The snapshot endoscopic Stokes imaging system setup

Supplemental Notes

1. Polarization effects of conventional endoscopes

Conventional endoscope consists of an objective lens, an imaging relay system comprising several rod lenses, an ocular lens and two sapphire windows permanently welded at both ends of the endoscope (see Figure S1A). The objective lens has a small entrance pupil (about 0.6mm diameter) and a large AFOV (typically over 70°) depending on specific applications. The ocular lens is designed with a very small chief ray angle (about 7°) and proximally infinite focus in the image space to accommodate the human eye or camera with a coupling lens[Error! Reference source not found.].

To investigate the polarization effects of conventional endoscopes, we analyzed four representative commercial endoscope models from Storz, Olympus, ShenDa and Omec (0° viewing angle). The measurements were conducted with a benchtop Mueller imaging system (see Note S7 & S8). The Mueller matrices were subsequently decomposed into diattenuation, retardance and depolarization scalars[2] (Figure S1B-E). The diattenuation was weak in all models (<0.05) and was omitted in the article. Based on the retardance and depolarization image patterns, the models can be categorized into two types: Type I (including Storz, ShenDa and Omec, Figure S1B, D & E) with centrosymmetric retardance patterns and radially increasing depolarization; Type II (Olympus, Figure S1C) with asymmetric retardance pattern and nearly evenly distributed depolarization across the FOV.

To demonstrate the incompatibility between conventional endoscopes and PG imaging due to the prominent polarization effects, the endoscopic PG imaging system was used to image a test target (a diffuser behind a linear polarizer, see Note S9). An effective PG imaging system should prevent crosstalk between the co- and cross-polarization imaging channels. We adapted both Type I (Storz) and II (Olympus) endoscopes, as well as the experimental endoscope that is custom-made without sapphire windows

(used as a benchmark), to the endoscopic PG imaging system to demonstrate the crosstalk (see Note S20) introduced by each. As shown in Figure S1F, the benchmark system showed negligible channel crosstalk ($\overline{ER} = 70.69$), about 40 times better when either the Type I ($\overline{ER} = 1.90$) or II ($\overline{ER} = 1.67$) endoscope was used. Specifically, the Type I model presented dispersive artifacts arising from retardance while the Type II model showed nearly homogeneous crosstalk in the FOV due to its intense depolarization (Figure S1C).

To evaluate how polarimetric imaging is affected by the depolarization of conventional endoscopes, we used the endoscopic Mueller imaging system with the experimental endoscope (its depolarization was controlled by changing the sapphire window) to measure the polarization properties of air (see Note S14, Figure S13, S14). As its depolarization increased from 0 to 0.7, the endoscopic Mueller imaging system became progressively degraded. This was evidenced by the substantial rise in the condition number of the experimental endoscope Mueller matrices, which indicates the backward stability of a Mueller polarimetric system. The reconstruction errors in diattenuation, retardance and depolarization increased almost exponentially with the depolarization of the experimental endoscope (see Note S21 and Figure S1G). The median depolarization of the representative Type I and II endoscopes were 0.22 (Omec), 0.15 (ShenDa), 0.20 (Storz) and 0.56 (Olympus) respectively. For the most popular Storz and Olympus endoscopes, their median depolarization corresponded to approximately three- and eight-fold reconstruction errors compared to the situation where the depolarization was around zero. Considering that polarimetry relies on precise measurements of the polarization properties of samples, the depolarization of the conventional endoscope poses challenges for polarimetric endoscopy.

2. Factors that decide the polarization effects of the conventional endoscopes

Given that both retardance and depolarization of endoscopes became negligible following the removal of sapphire windows[8], we assumed that factors including the optic axis (OA) direction and thickness (T) of the sapphire window, the AFOV of the

endoscope, the central wavelength (CWL) and bandwidth (measured by the full width at half maximum, FWHM) of the illumination light, and the position of the sapphire window (i.e. the distal and proximal ends) affect the polarization effects. The assumption was verified through experiments (Figure S2-S5) and the influence of these key factors was examined. The experimental results reveal the following facts. First, the patterns of the retardance and depolarization were primarily determined by the OA direction. The C-cut featured almost identical patterns to the Type I endoscope. The R-cut exhibited consistent patterns with the Type II endoscope. The A-cut window induced hyperbolic retardance fringes and nearly evenly distributed depolarization. Second, the sapphire window position (distal/proximal) had substantial influence in the polarization effects. Installing the sapphire window only at distal end resulted in complex retardance patterns. Conversely, placing the sapphire window only at the proximal end yielded simple effects: negligible polarization effects for the C-cut and almost homogeneous retardance and depolarization for the A-cut. Using C-cut windows at both ends was essentially the same as using a C-cut window at the distal end only. Third, the impact of the window thickness and AFOV were similar. Thicker windows, larger AFOV generally led to stronger retardance represented by more orders in the retardance image and higher depolarization. Fourth, the polarization effects were highly wavelength and bandwidth dependent. Longer wavelength corresponded to weaker retardance and lower depolarization. The bandwidth slightly influenced retardance but strongly influenced the depolarization. Depolarization was still considerable even using a single-frequency laser, suggesting part of depolarization was bandwidth insensitive.

3. Formation mechanism of the retardance in conventional endoscopes

Because of the birefringence of the sapphire window, a randomly polarized incident ray will be split into the orthogonally polarized ordinary and extraordinary ray pair whose SOPs are perpendicular to each other if the ray did not incident along the OA direction. The ordinary ray undergoes regular refraction and its optical path can be calculated with Snell's law. In contrast, the refraction of the extraordinary ray in the sapphire window is more complicated, but its optical path can still be calculated using the Huygens's

principle[4]. In the simulation, the object was assumed to be at infinity and thus only the primary ray corresponding to a unique field angle was considered for a specific object point in the FOV. As the ray passed through the sapphire window, a phase difference was induced between two rays due to the birefringence of the window, and lead to retardance. Let the direction cosine vector of the ordinary ray and the OA be $[\xi_o \quad \eta_o \quad \zeta_o]^{\mathrm{T}}$ and $[\alpha \quad \beta \quad \gamma]^{\mathrm{T}}$, and the refractive indices for the ordinary and extraordinary rays be n_o and n_e respectively. The direction cosine vector of the extraordinary ray can be calculated by

$$\begin{bmatrix}\xi_e\\ \eta_e\\ \zeta_e\end{bmatrix} = \frac{1}{\delta_{eg}}\begin{bmatrix} n_o^2(n_e^2+N\beta^2) & -n_o^2N\alpha\beta & 0\\ -n_o^2N\alpha\beta & n_o^2(n_e^2+N\alpha^2) & 0\\ 0 & 0 & \Gamma\Delta/\zeta_o\end{bmatrix}\begin{bmatrix}\xi_e\\ \eta_o\\ \zeta_o\end{bmatrix} - \frac{\gamma N\Delta}{\delta_{eg}}\begin{bmatrix}1&0&0\\0&1&0\\0&0&0\end{bmatrix}\begin{bmatrix}\alpha\\ \beta\\ \gamma\end{bmatrix} \tag{1}$$

where

$$\delta_{eg}^2 = n_e^2[n_o^2\Gamma^2 - N(\gamma\Delta + n_o^2a)^2], \qquad \Gamma = n_e^2 + N(1-\gamma^2), \qquad \Delta^2 = \Gamma\delta_o^2 + n_o^2Na^2,$$

$$N = n_o^2 - n_e^2, \qquad \delta_o^2 = n_e^2 - n_o^2(1-\xi_o^2), \qquad a = \alpha\xi_o + \beta\eta_o$$

Due to the difference in the refractive indices and the optical paths, a phase shift between the pair of perpendicularly polarized rays is introduced. The phased shift can be calculated by[5]:

$$\delta = \frac{2\pi T}{\lambda}(n_o\cos\theta_o - n_e\cos\theta_e) \tag{2}$$

where δ is the phase shift, T is the sapphire window thickness, λ is the wavelength, $\delta_{o,e}$ are the refraction angles of the ordinary and extraordinary rays. Moreover, since the sapphire is a negative uniaxial crystal (i.e. $n_o > n_e$), the effective refractive index of the extraordinary ray, n_e, is dependent on the incident direction of the ray and need to be calculated with the index ellipsoid of the sapphire. Denoting the length of the minor axis and equator radius of the ellipsoid by n_E and n_O respectively, n_e can be calculated by[6]:

$$\frac{1}{n_e^2} = \frac{\cos^2\phi}{n_O^2} + \frac{\sin^2\phi}{n_E^2} \tag{3}$$

where ϕ is the angle between the incident ray and the OA. Furthermore, the

polarization direction of the ordinary ray is perpendicular to the plane defined by the incident ray and the OA, while the extraordinary ray is polarized perpendicular to the polarization direction of the ordinary ray and the propagation direction of the incident ray.

Knowing the phase shift (δ) and the polarization direction of the extraordinary ray component (θ), the Mueller matrix corresponding to the ray can be calculated by:

$$\mathbf{M} = \begin{bmatrix} 1 & 0 & 0 & 0 \\ 0 & \cos^2 2\theta + \cos\delta \sin^2 2\theta & (1-\cos\delta)\sin 2\theta \cos 2\theta & -\sin\delta \sin 2\theta \\ 0 & (1-\cos\theta)\sin 2\theta \cos 2\theta & \sin^2 2\theta + \cos\delta \cos^2 2\theta & \sin\delta \cos 2\theta \\ 0 & \sin\theta \sin 2\theta & -\sin\delta \cos 2\theta & \cos\delta \end{bmatrix} \quad (4)$$

To derive the retardance in the entire FOV, the retardance for the primary rays of each object point in the FOV was calculated. Notably, each object point is projected onto the image plane via different optical paths corresponding to a different effective birefringence, thereby spatially inhomogeneous retardance manifested in the FOV.

4. Simulate the retardance in conventional endoscopes

The retardance effects of the endoscope with a sapphire window at the distal end were simulated with MATLAB 2022b environment (Figure 1B-E). In the simulation, the spatial relation of the rays and the sapphire window was defined by the 3D Cartesian coordinates. The surface normal of the window was assumed along the *z*-axis (i.e. its direction cosine vector is $[0 \quad 0 \quad 1]^{\mathrm{T}}$) and the OA direction was defined by the azimuth angle (θ) in the *x*-*o*-*y* plane and zenith angle (ϕ) between the OA and the z-axis (i.e. its direction cosine vector is $[\cos\theta \sin\phi \quad \sin\theta \sin\phi \quad \cos\phi]^{\mathrm{T}}$, see Figure S15). To simulate the retardance pattern for the C-, A- and R-cut windows, their OA directions were set as $[0 \quad 0 \quad 1]^{\mathrm{T}}$, $[1 \quad 0 \quad 0]^{\mathrm{T}}$ and $[0.64 \quad 0 \quad 0.77]^{\mathrm{T}}$ respectively. The thickness of the windows was set to 1 mm. The illumination light was set as 532 nm monochromatic, and the AFOV was set to 80°. With these parameters set, a $512 \times 512 \times 3$ array was created to represent the directions of the primary rays propagating from the OPs to the sapphire window, and from the center to the edge of the array, the

zenith angles of the rays were varied from 0° to 35° while the azimuth angle rotates around the z-axis (Figure S15). Then the Mueller matrix for each ray across the AFOV can be calculated following equation (1)-(4). In the calculation, the refractive indices for the ordinary and extraordinary rays were adopted from existing literature[7]. By decomposing the Mueller matrix for each ray in the 512×512 field, the retardance images were obtained (Figure 1B). The rest retardance patterns (Figure 1C-E) were then simulated following the same procedure by singly altering the thickness from 1 mm to 2 / 2.8 mm, the AFOV from 80° to 65° and wavelength from 532 nm to 630 nm respectively.

5. Formation mechanism of the chromatic depolarization and the simulation

Since the sapphire window induced retardance is wavelength dependent, the incoherent superposition of light retarded depending on the wavelength leads to the chromatic depolarization. Therefore, the resulting Mueller matrix ($\mathbf{M}_S$) for broadband illumination can be calculated by

$$\mathbf{M}_S = \int \mathbf{M}(\lambda)\,\mathrm{PSD}(\lambda)d\lambda \tag{5}$$

where $\mathbf{M}(\lambda)$ denotes the Mueller matrix at wavelength λ and $\mathrm{PSD}(\lambda)$ denotes the power spectral density of the illumination light.

To simulate the chromatic depolarization, we assumed the power spectral density was uniformly distributed from 400 nm to 700 nm. The refractive indices were fitted based on the data provided by previous study[7] (Figure S6). To calculate the final Mueller matrix, Mueller matrices in the FOV were calculated from 400 to 700 nm with 1 nm separation; the thickness of the sapphire windows were set to 1 mm and AFOV were 80°. The final Mueller matrix ($\mathbf{M}_S$) was calculated by

$$\mathbf{M}_S = \sum_{\lambda=400}^{700} \mathbf{M}(\lambda) \Big/ 300 \tag{6}$$

The chromatic depolarization is then obtained by decomposing $\mathbf{M}_S$.

6. Formation mechanism of the aperture depolarization and the simulation

Since the OPs on the object emit a cone of rays whose opening angle is defined by the aperture of the endoscope, the incoherent superposition of the rays in the cone at the image plane results in the aperture depolarization. Similar to the chromatic depolarization, the Mueller matrix ($\mathbf{M}_{\mathrm{ap}}$) of each point in the FOV concerning the ray cone can be calculated by:

$$\mathbf{M}_{\mathrm{ap}} = \int \mathbf{M}(\theta)\,\mathrm{DF}(\theta)d\theta \tag{7}$$

where $\mathbf{M}(\theta)$ denotes the Mueller matrix corresponding to the ray in direction θ in the ray cone and $\mathrm{DF}(\theta)$ denotes the density function for ray distribution in the cone.

To simulate the aperture depolarization, the ray density in the cone was assumed uniform, and a $64 \times 64 \times 3$ array was created for each primary in the FOV represented by the $512 \times 512 \times 3$ array to represent the directions of rays that deviate from the primary ray in the cone. Additionally, the F number of the endoscope was assumed to be 5.72 (usually ranging from 5 to 9 for conventional endoscopes) and 80° AFOV, resulting in 10° aperture angle at the center of the FOV and 5.88° at the edge. Besides, the sapphire window thickness was assumed 1 mm and the wavelength was assumed at 532 nm. The Mueller matrix of a point in the FOV concerning the ray cone was then calculated by

$$\mathbf{M}_{\mathrm{ap}} = \sum_{\theta}^{N} \mathbf{M}(\theta) \Big/ N \tag{8}$$

where N denotes the total number of rays assumed in the cone. The aperture depolarization was then obtained by decomposing $\mathbf{M}_{\mathrm{ap}}$.

7. Simulate the polarization effects when mismatches occur between the sapphire and compensation plates

The Mueller matrix of the endoscope when mismatches occur between the sapphire and compensation plates can be calculated by directly multiplying the Mueller matrices of the endoscope when the two plates are mounted singly at the distal end. The total

Mueller matrix can be simply obtained because the rays keep their propagation direction after passing through the plane-parallel plate and the ordinary and extraordinary rays will not further split into ray pairs in the compensation plate for either C- or A-cut options.

In the simulation, we assumed the light spectrum ranges from 400 to 700 nm, the AFOV to be 80°, the thickness of the MgF_2 compensation plate as 1 mm, the OA direction as $[0 \quad 0 \quad 1]^T$ and $[1 \quad 0 \quad 0]^T$ for C- and A-cut plates. The aperture depolarization is ignored in the simulation because it is weak comparing to the chromatic depolarization in broadband situation and including the aperture depolarization in the simulation is time consuming.

Then, we firstly find the optimal thickness of the C- and A-cut sapphire windows that minimizes the retardance in the FOV. Here, only the retardance is considered to obtain the optimal ratios, since the depolarization is its secondary effect. With the optimal thickness (2.29 mm for C-cut, 2.43 mm for A-cut) obtained, we increased the thickness of the sapphire window by 0.01 mm for each step and calculated the resulting polarization effects. Moreover, the OAs of the sapphire windows were assumed ideally matched with the compensation plate when the thickness mismatch is examined. Secondly, for OA mismatch, we adopted the optimal thickness for the plates and changed their OAs to examine the resulting polarization effects. In the simulation, we only change the OA direction in the zenith angle because the mismatch in the azimuth angle mismatch can be mitigated by rotating the sapphire window in practice.

8. The benchtop Mueller imaging system

The setup of the benchtop Mueller imaging system is illustrated in Figure S13. The system, in general, was composed by the polarization state analyzer (PSA) and the polarization state generator (PSG).

The PSA was composed sequentially of a coupling lens (AC254-050-A-ML, Thorlabs),

a two-position slider (CFS1/M, Thorlabs) with a QWP (WP140HE, Edmund) installed in one position with the fast axis oriented at random direction and a polarized monochrome camera (PHX050S-PC, LUCID) with the classic micro polarizer array (MPA) whose superpixel is composed by 0°, 45°, 90° and 135° micro polarizers. By sliding the two-position slider for each measurement, the PSA functions as a two-snapshot full-Stokes polarimeter.

The PSG consists of a light source, a diffuser (a piece of white paper), an LP (WP140HE, Edmund) whose transmission axis was fixed aligning with the 0° micro polarizers in the polarized camera of the PSA, and a QWP (XP42HE, Edmund) installed in a rotation mount. During the measurement, the QWP was rotated counterclockwise to aim its fast axis at 0°, 30°, 60° and 135° sequentially with respect to the transmission axis of the LP to minimize the systematic error[8].

To measure the Mueller matrices of the endoscopes, the benchtop Mueller imaging system was calibrated using the eigenvalue calibration method[9] to acquire the accurate generator matrix ($\mathbf{G}$) of the PSG and the analyzer matrix ($\mathbf{A}$) of the PSA. In the measurement, the PSG generates four distinct SOPs sequentially by rotating the QWP in the PSG. $\mathbf{G}$ is thus a 4×4 matrix composed by the four 4×1 Stokes vectors corresponding to the four SOPs. The PSA provides eight 1×4 analyzer vectors corresponding to the four micro polarizers with and without the QWP in front of the camera forming the 8×4 $\mathbf{A}$. Therefore, totally 32 intensities measurements, which can be organized into an 8×4 intensity matrix ($\mathbf{I}$), were carried out by the system for a complete Mueller matrix imaging:

$$\mathbf{I} = \mathbf{A}\mathbf{M}_\mathrm{e}\mathbf{G} \tag{9}$$

and the Mueller matrix of the endoscope ($\mathbf{M}_\mathrm{e}$) can be calculated by inverting equation (9):

$$\mathbf{M}_\mathrm{e} = \mathbf{A}^{+}\mathbf{I}\mathbf{G}^{+} \tag{10}$$

where + denotes the pseudoinverse.

9. Measure the polarization effects of the endoscopes with benchtop Mueller imaging system

In this work, the benchtop Mueller imaging system was adopted to measure the polarization effects of (1) the representative conventional endoscopes, (2) the experimental endoscope with various sapphire windows and illumination light sources to determine the influence of the key factors, and (3) the PME prototype, the experimental endoscope without sapphire windows. To measure the polarization effects of these endoscopes, they were placed between the PSG and PSA and the system was adjusted to focus on the diffuser of the PSG (Figure S13).

Firstly, the commercially sourced representative conventional endoscopes were model 26003AA from Karl Storz, model WA53000A from Olympus, model J0800B from ShenDa and model 680-331000H from Omec. In the experiment, a white light source (LED-D1-MAX6K, Oeabt) with 200 nm FWHM was adopted by the PSG of the benchtop system and its spectra is provided in Figure S16.

Secondly, to determine the influence of the OA direction and the position of the sapphire window on the polarization effects of the conventional endoscope, 1 mm A-, C- and R-cut sapphire windows were mounted at both ends of the experimental endoscope individually and simultaneously, and the resulting polarization effects were measured. In the experiments, the AFOV of the endoscope was 80°, and a narrowband light source whose CWL was 532 nm and FWHM was 10 nm (spectra provided in Figure S16) was adopted by the PSG. The light source was constructed by the white light source (LED-D1-MAX6K, Oeabt) and a bandpass filter (BP532-10nm, RAYAN TECHNOLOGY).

To determine the influence of the thickness of the sapphire window and the CWL and the bandwidth of the illumination light on the polarization effects of the conventional endoscope, C-cut windows of 0.5 mm, 1 mm and 2 mm thickness and A-cut windows of 1 mm and 2.8 mm thickness were mounted at the distal end of the experimental

endoscope sequentially to measure the resulting polarization effects with various light sources. The AFOV of the endoscope was 80° and the light sources adopted in the PSG include the white light source (LED-D1-MAX6K, Oeabt) whose FWHM is 200 nm, the single longitudinal mode laser (opus 532, Novanta Photonics) whose CWL and FWHM are 532 nm and 0.6 nm, the green LED light source (HI-080, HengYang) whose CWL and FWHM are 532 nm and 30 nm, and three narrowband light sources whose CWLs are 435 nm, 532 nm and 630 nm and FWHMs are 10 nm. The narrowband light sources were constructed by the white light source (LED-D1-MAX6K, Oeabt) and three bandpass filters (BPH435-10nm, BP532-10nm, BPH630-10nm, RAYAN TECHNOLOGY). The spectra of the light sources are provided in Figure S16, and the measurement results are provided in Figure S3-S5.

Thirdly, to measure the polarization effects of the PME and the experimental endoscope without sapphire windows, the white light source (LED-D1-MAX6K, Oeabt), the green LED light source (HI-080, HengYang) and the narrowband light source constructed by the white light source (LED-D1-MAX6K, Oeabt) and a bandpass filter (BP532-10nm, RAYAN TECHNOLOGY) were adopted by the PSG, the AFOV of the endoscopes were limited to 70°. Additionally, the model J0800B from ShenDa was also measured with the same condition for comparison (Figure S7).

10. The endoscopic polarization-gated imaging system and the PG-WLE system

The setup of the polarization-gated imaging system is presented in Figure S17. The system included two parts: the illumination module and the imaging module. The illumination module is composed by the white light source (LED-D1-MAX6K, Oeabt), a diffuser (a piece of white paper) and an LP (WP140HE, Edmund). The imaging module is composed of an endoscope, a coupling lens (AC254-050-A-ML, Thorlabs) and a polarized color camera (BFS-U3-51S5PC-C, Teledyne FLIR).

As presented in Figure 4A, the setup of the PG-WLE system was very similar to the imaging module of the endoscopic polarization-gated imaging system except that the

endoscope was replaced by the PME, an LP (XP42HE, Edmund) whose transmission axis was aligned with the 90° micro polarizers of the polarized camera was mounted at the distal end of the PME, and the illumination light was guided from an endoscopic LED light source (RFFM-16A5, Rayfine, the spectrum is provided in Figure S16) to the light port of the PME by a fiber bundle (495NCSC, Storz).

11. Calculating the extinction ratio from the Mueller matrix

In Figure 2R, the extinction ratios of the endoscopes are calculated from their Mueller matrices. In the calculation, the illumination light was assumed to be horizontally polarized (i.e.$\vec{\mathbf{S}}_{\text{in}} = [1 \quad 1 \quad 0 \quad 0]^{\text{T}}$) and the analyzer vector for the co- and cross-polarization channels were thus $\vec{\mathbf{A}}_{\text{co}} = [1 \quad 1 \quad 0 \quad 0]$ and $\vec{\mathbf{A}}_{\text{cross}} = [1 \quad -1 \quad 0 \quad 0]$. Knowing the Mueller matrix of the endoscope ($\mathbf{M}_{\text{e}}$), the co- and cross-polarization intensities can be calculated as:

$$\text{I}_{\text{co/cross}} = \vec{\mathbf{A}}_{\text{co/cross}} \mathbf{M}_{\text{e}} \vec{\mathbf{S}}_{\text{in}} \tag{11}$$

The extinction ratio is thus

$$\text{ER} = \frac{\text{I}_{\text{co}}}{\text{I}_{\text{cross}}} \tag{12}$$

The ER of each point in the FOV is then averaged to obtain the final result.

12. Specular highlight removal experiments

The *in vivo* specular highlight removal experiment was carried out with the PG-WLE system.

Firstly, the oral cavity of a volunteer was imaged by the PG-WLE system to obtain the 0°, 45°, 90° and 135° subimages. Since the illumination light was polarized in the 90° direction, the 90° subimage was the co-polarization image and the 0° subimage was the cross-polarization image where the specularities were removed. The four subimages were then added together to obtain the color-resolved-only WLE images:

$$\text{I} = (\text{I}_0 + \text{I}_{45} + \text{I}_{90} + \text{I}_{135})/2 \tag{13}$$

The WLE images were then fed into the computation-based specular highlight removal algorithms. Furthermore, with the polarized subimages, the PD images can be calculated by:

$$I = \frac{I_{co} - I_{cross}}{I_{co} + I_{cross}} = \frac{I_{90} - I_0}{I_{90} + I_0} \quad (14)$$

For the images presented in Figure 4N, the PD images for the red, green and blue color channels were calculated separately and then merged together with a pseudocolor scheme.

Next, we replaced the PME in the PG-WLE system with a conventional endoscope (J0800B, ShenDa) and repeated the procedure to obtain results for the comparison (Figure 3P).

13. PHP

The PHP is defined by the percentage of the specular highlight pixels in the image[10], and is adopted here to assess the specular highlight removal effectiveness. To avoid missing the specular highlight pixels in the image, which is a common issue for current image processing algorithms, we manually segmented the image into subimages containing the specular highlight pixels and then picked out the specular pixels by thresholding.

14. Surgical smoke removal experiments

The *in vivo* surgical smoke removal experiment was conducted with the PG-WLE system. The experimental setup and data collection procedure for this experiment were the same as the specular highlight removal experiment.

In the experiment, we firstly imaged the abdomen of a lab mouse blurred by smoke generated by an electric knife on adipose tissue. With the co- and cross-polarization images, the smoke-removed images (J) can be calculated by:

$$J = \frac{I_{co} + I_{cross} - A}{t} + A \quad (15)$$

where A is a constant representing the environment brightness which is the intensity image of the scene that can be measured when the scene is completely obscured by the smoke, and t is the transmission rate that can be calculated by:

$$t = 1 - \frac{I_c}{A} \tag{16}$$

where I_c is a linear combination of the 0°, 45° and 90° subimages that minimizes the smoke blurry in the image[11].

In the experiment, the images were acquired at the frequency of 20 frames/s. The images were processed off-line, and the RPD algorithm was implemented in MATLAB 2023 on a laptop with an Intel Core i7-2700H processor. The processing time for a single polarization image was approximately 2.6 seconds.

15. The endoscopic Mueller imaging system

The setup of the endoscopic Mueller imaging system is presented in Figure S18. The system was essentially the same as the benchtop Mueller imaging system except that an endoscope was attached to the PSA. Therefore, the imaging procedure of the endoscopic system were the same as the benchtop system but the polarization effects of the endoscope need to be considered. In the experiment, the polarization effects of the endoscope in the system was considered as part of the total polarization effects of the target. Therefore, to obtain the original Mueller matrix of the target ($\mathbf{M_o}$), the Mueller matrix of the endoscope ($\mathbf{M_e}$) must be acquired first with the benchtop system, and $\mathbf{M_o}$ was then calculated by:

$$\mathbf{M_o} = \mathbf{M_t}\mathbf{M_e^+} \tag{17}$$

where $\mathbf{M_t}$ is the Mueller matrix denote the total polarization effects of the target measured by the endoscopic Mueller imaging system.

16. Measure the polarization properties of targets with the endoscopic Mueller imaging system

The system setups for the measurements are presented in Figure S18. The targets whose

polarization properties were measured by the endoscopic Mueller imaging system include: (1) the LP film (WP140HE, Edmund), (2) the QWP film (XP42HE, Edmund) and (3) the *ex vivo* porcine liver tissue. In the measurements, the white light source (LED-D1-MAX6K, Oeabt) was adopted. The PME, a conventional endoscope (J0800B, ShenDa) and the experimental endoscope without sapphire window (used as benchmark) were incorporated to the system for the measurement, and the AFOVs of the endoscopes were limited to 70°.

17. PIQE

The PIQE is a no-reference image quality metric that mimics human perception for real-world imagery[12]. The algorithm divides the input image into non-overlapping 16×16 subimages and then extracts the local features for image distortion assessment. In this work, the PIQE function provided by MATLAB 2022b was adopted to evaluate the quality of the polarimetric images.

18. Snapshot endoscopic Stokes imaging system

The setup of the system is presented in Figure S19. The illumination light is guided to the endoscope from the endoscopic cold light source (RFFM-16A5, Rayfine) via a fiber bundle (495NCSC, Storz), and the illumination light is polarized by a circular polarizer (CP42HE, Edmund) mounted at the distal end of the endoscope to generate fully circularly polarized light. The PSA of the system consisted of a coupling lens (AC254-075-A-ML, Thorlabs), a non-polarizing 50:50 beamsplitter (CCM1-BS013/M, Thorlabs), a QWP (WP140HE, Edmund), two polarized monochrome cameras (PHX050S-PC, LUCID) and an endoscope. In the PSA, the coupling lens is placed behind the proximal end of the endoscope and followed by the beamsplitter. The QWP is randomly oriented and installed in front of one of the polarization cameras so that all Stokes parameters can be obtained by one snapshot.

19. Polarimetric endoscopic imaging of the oral vestibule

The snapshot endoscopic Stokes imaging system was applied to measure the

polarization effects of the oral vestibule of a volunteer. The PSA of the system provides eight analyzer vectors (8×4 $\mathbf{A}$) to obtain the 8×1 intensity vector:

$$\vec{\mathbf{I}} = \mathbf{A}\vec{\mathbf{S}} \tag{18}$$

The complete Stokes vector of the light ($\vec{\mathbf{S}}$) returning from the tissue can be obtained by inverting equation (18):

$$\vec{\mathbf{S}} = \mathbf{A}^{+}\vec{\mathbf{I}} \tag{19}$$

Like the endoscopic Mueller imaging system, the Mueller matrix of the endoscope ($\mathbf{M}_{\mathrm{e}}$) Must be divided from $\vec{\mathbf{S}}$ to obtain the original Stokes vector ($\vec{\mathbf{S}}_{\mathrm{o}}$) of the light returning from the scene:

$$\vec{\mathbf{S}}_{\mathrm{o}} = \mathbf{M}_{\mathrm{e}}^{+}\vec{\mathbf{S}} \tag{20}$$

For the polarization effects of the oral vestibule, since it typically exhibits mainly linear retardance and depolarization with negligible diattenuation[13], the linear polarized components of the light are converted by the retardance of the tissue given that the illumination light is fully circularly polarized. Therefore, the retardance of the tissue can be obtained by calculating the degree of linear polarization of the light:

$$\mathrm{R} = \sqrt{s_1^2 + s_2^2}/s_0 \tag{21}$$

Similarly, the depolarization of the tissue can be represented by the loss of degree of circular polarization of the light:

$$\Delta = 1 - |s_3|/s_0 \tag{22}$$

20. Crosstalk between the co- and cross-polarization channels

The endoscopic polarization-gated imaging system was utilized in the experiment to demonstrate the crosstalk between the co- and cross-polarization channels caused by the polarization effects of the conventional endoscope (Figure S1F). In the experiment, the illumination module of the system generated linearly polarized light (polarization direction was aligned with the 0° micro polarizers in the polarized color camera). A type I (26003AA, Storz), a Type II (WA53000A, Olympus) and the experimental endoscope without sapphire windows (benchmark) were incorporated to the system

sequentially for the experiment, and the endoscopes were adjusted to focus on the diffuser in the illumination module. The 0° and 90° subimages were obtained as the co- and cross-polarization images.

21. Measure the polarimetric imaging error depending on the depolarization of the endoscope

The polarimetric imaging error caused by the depolarization of the endoscope is measure by the following steps: (1) use the benchtop Mueller imaging system to obtain the Mueller matrix of the experimental endoscope ($\mathbf{M}_e$) with the 2 mm C-cut sapphire window installed at the distal end and illuminated by the white light source (LED-D1-MAX6K, Oeabt); (2) decompose the Mueller matrix of the endoscope; (3) create the index map from the depolarization image that sorts out the points with depolarizations close to 0, 0.1, …, 0.7 (within ± 0.02) in the FOV; (4) calculate the condition number of the Mueller matrix of each point in the FOV; (5) incorporate the experimental endoscope to the endoscopic Mueller polarimetric imaging system and measure the Mueller matrix of the air (i.e. empty field, focused on the diffuser of the PSG, $\mathbf{M}_a$); (6) divide $\mathbf{M}_a$ by $\mathbf{M}_e$ and decompose the resultant Mueller matrix to obtain the diattenuation, retardance and depolarization of the air (since air has no polarizing effects, the remaining polarization properties were caused by the endoscope); (7) sort out the condition number, diattenuation, retardance and depolarization of the air with the index map, and calculate the average values depending on the depolarization of the endoscope. The process is presented in Figure S14.

22. The retardance order

The retardance order is a metric used here to assess the centrosymmetric and periodic retardance effects induced into the FOV by the C- and A-cut sapphire windows of the endoscopes. To calculate the retardance order, the retardance of the central point of the FOV was set as 0. The pixelated variation from the center to the edge along the radius was summed up to obtain the total retardance variation. The retardance order of the point on the edge is then obtained by dividing the total retardance variation by 2π:

$$RO(\vec{r}) = \frac{1}{2\pi}(|R_1 - R_0| + |R_2 - R_1| + \cdots + |R_n - R_{n-1}|) \quad (23)$$

where $RO(\vec{r})$ is the retardance order of a point on the edge whose relative position to the central point is denoted by $\vec{r}$, R_n denotes the retardance of the *n*th pixel on the track from the center to the point on edge, and R_0 is the retardance of the central point. Additionally, since the measured retardance patterns were often eccentric, we calculated the retardance order for every point on the edge and use their mean value as the final retardance order.

23. Sample preparation for biomedical imaging

In this study, biomedical samples used in the experiments include: (1) a piece of porcine liver tissue, (2) a lab mouse and (3) the oral cavity of a volunteer. The *ex vivo* porcine liver tissue used in the endoscopic polarimetric imaging experiment was commercially sourced and used as an imaging sample within ten hours after separated from the pig. The lab mouse used in the surgical smoke removal experiment was an eight-week-old male ICR mouse that weighted 20-30 g. In the experiment, the mouse was anesthetized and its abdomen was then cut open for the imaging experiment, and the experiment was finished within 0.5 hours. The volunteer for oral cavity imaging experiments was a healthy 31-year-old male. The endoscopes were disinfected beforehand, and the experiment did not involve any injury, drug or any potentially harmful Method. The ethics approval for this study was granted by Ethics Committee at Zhejiang lab (reference number: ZJSL-2022-9).

Supplemental Figures

1. Polarization effects of conventional endoscopes and their influence on polarization-resolved endoscopy

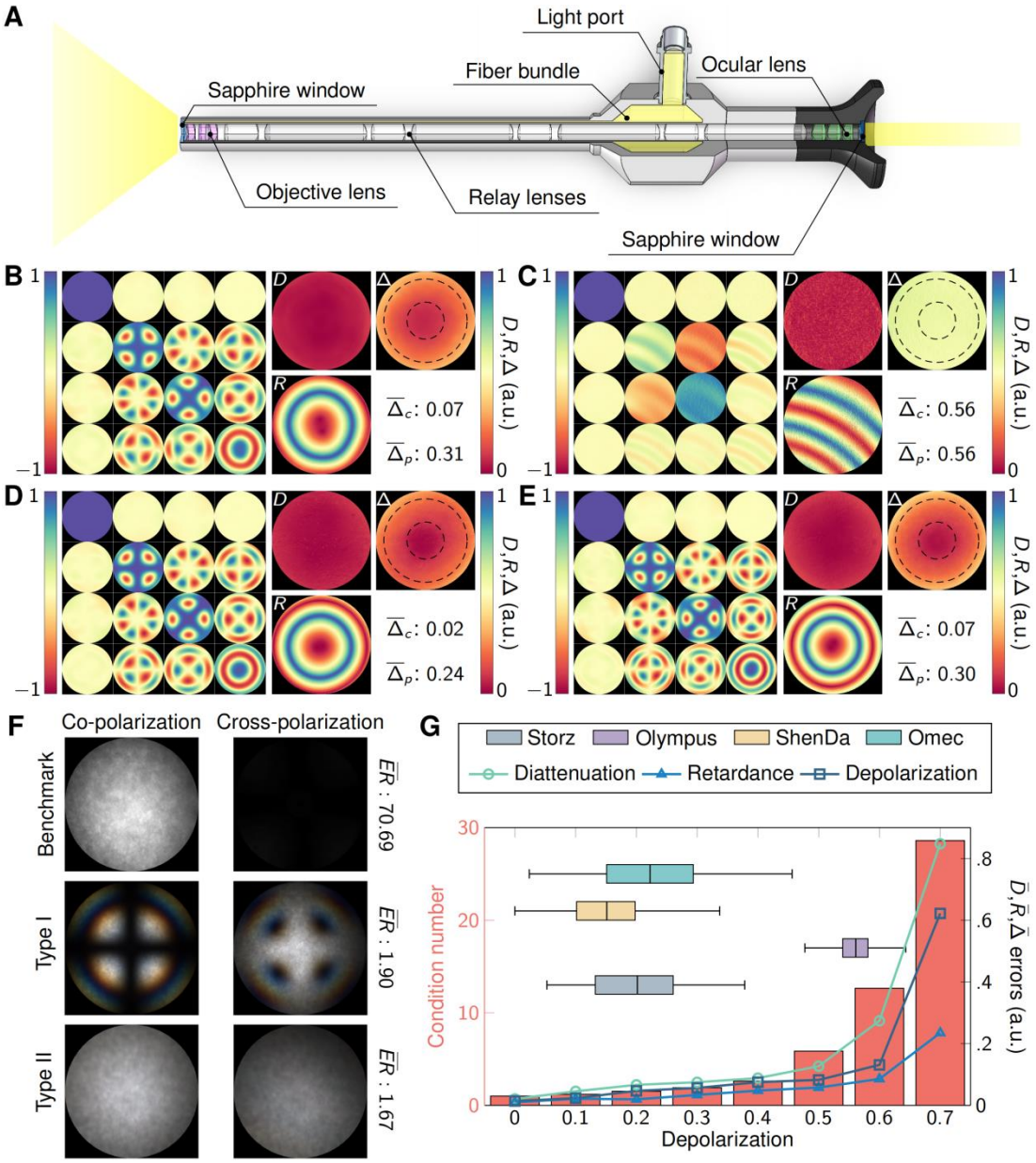

Figure S1. Polarization effects of conventional endoscopes and their influence on polarization-resolved endoscopy. A, Typical design of a conventional endoscope for surgery. **B-E**, The Mueller matrices and diattenuation (D), retardance (R) and depolarization (Δ) images of the conventional endoscopes from Storz (**B**), Olympus (**C**), ShenDa (**D**) and Omec (**E**). The average depolarization of the central ($\overline{\Delta}_c$) and the peripheral ($\overline{\Delta}_p$) regions were calculated from the areas inside and outside the inner dashed circles respectively in the depolarization images. **F**, The co- and cross-polarization images obtained by the endoscopic polarization-gated imaging system with the experimental endoscope without sapphire windows (Benchmark), the Type I (Storz) and the Type II (Olympus) endoscope, and their average extinction ratios ($\overline{ER}$) within the FOV. **G**, The barchart shows the condition number of the endoscope Mueller matrices depending on the depolarization level of the endoscopes, and the line graph

shows the corresponding reconstruction errors for diattenuation ($\bar{D}$), retardance ($\bar{R}$) and depolarization ($\bar{\Delta}$). The horizontal boxplots indicate the depolarization distributions of the four representative conventional endoscopes in the FOV.

2. Factors influencing the polarization effects of the conventional endoscopes

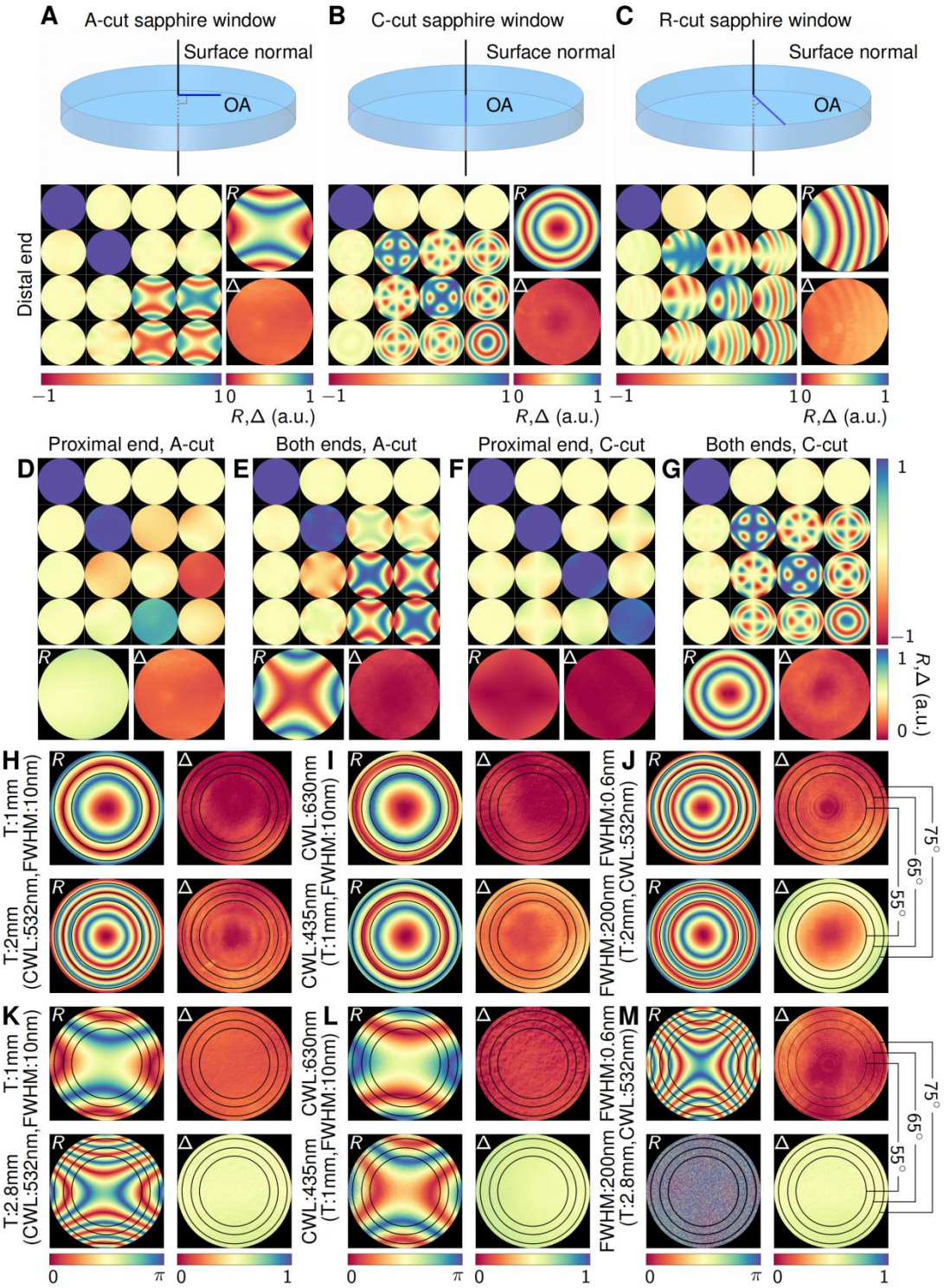

Figure S2. The factors influencing the polarization effects of the conventional endoscopes. A-C. Polarization effects of the experimental endoscope with the A-, C- and R-cut sapphire windows mounted at the distal end. **D-G.** Polarization effects of the experimental endoscope with A- or C-cut sapphire windows mounted at the proximal end or both ends. In these experiments, the thicknesses of the sapphire windows were all 1 mm; the light source had 532 nm CWL and 10 nm FWHM, and the AFOV of the endoscopes was 80°. **H-M.** The retardance and depolarization images measured from the experimental endoscope (**H**) when the C-cut sapphire windows have different thickness (1 mm VS 2 mm), illuminated by light with 532 nm CWL and 10 nm FWHM; (**I**) when the C-cut sapphire windows are under different central wavelengths (435 nm VS 630 nm), 10 nm FWHM, 1mm thick; (**J**) when the C-cut sapphire windows are under different bandwidth (200 nm VS 0.6 nm), 2 mm thick, 532nm CWL; (**K**) when the A-cut sapphire windows have different thickness (1 mm VS 2.8 mm), and illuminated by light with 532 nm CWL and 10 nm FWHM; (**L**) when the A-cut sapphire windows work under different central wavelengths (435 nm VS 630 nm), 10 nm FWHM, 1mm thick; and (**M**) when the A-cut sapphire windows are under different bandwidth (200 nm VS 0.6 nm), 2.8 mm thick, 532nm CWL.

3. Polarization effects of the conventional endoscope depending on the key factors

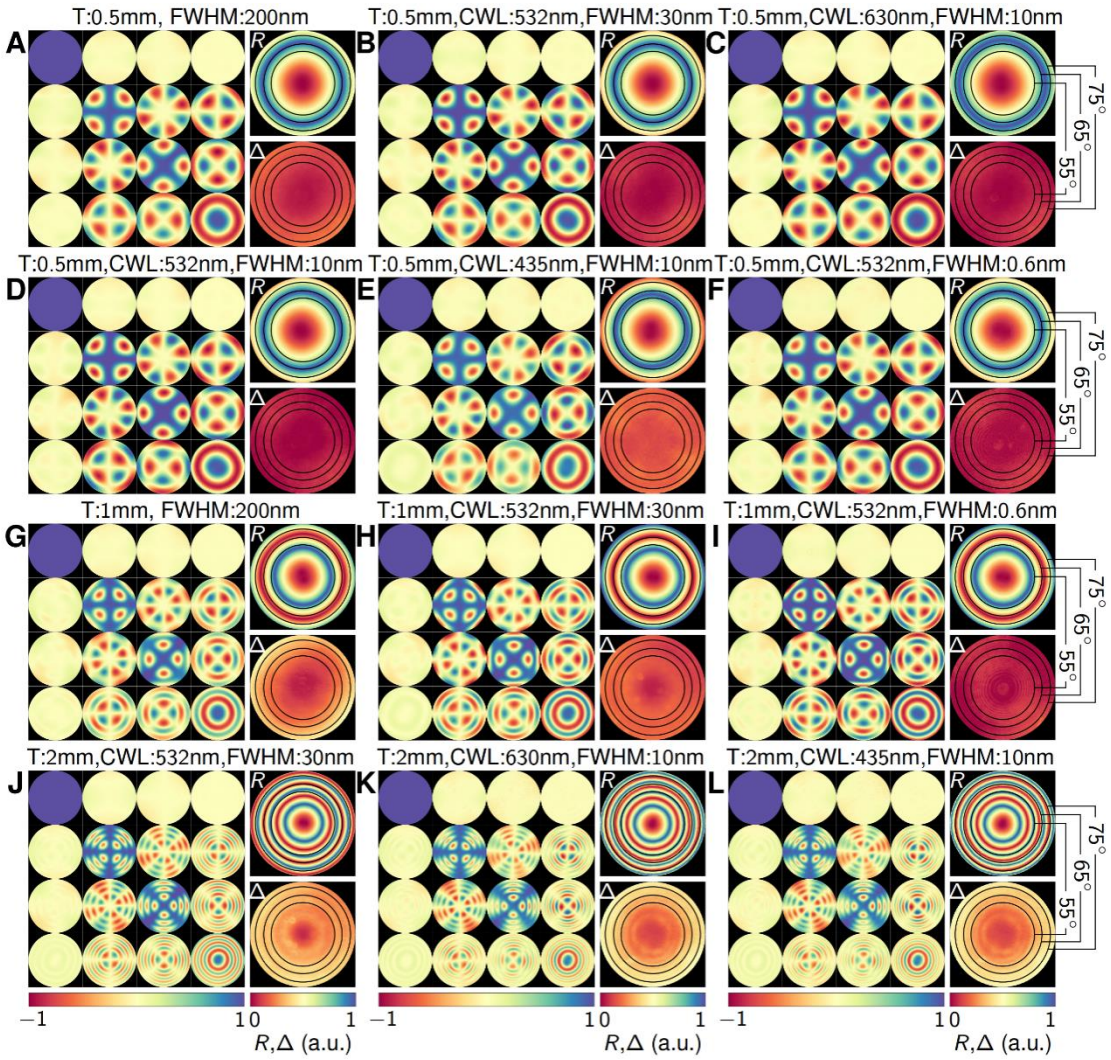

Figure S3. Polarization effects of the conventional endoscope depending on the key factors - full results (part I). Mueller matrices and retardance (*R*) and depolarization (Δ) images of the experimental endoscope when the sapphire window mounted at the distal end and the illumination light were: **A**, C-cut, T = 0.5 mm, FWHM = 200 nm (white light source); **B**, C-cut, T = 0.5 mm, CWL = 532 nm, FWHM = 30 nm; **C**, C-cut, T = 0.5 mm, CWL = 630 nm, FWHM = 10 nm; **D**, C-cut, T = 0.5 mm, CWL = 532 nm, FWHM = 10 nm; **E**, C-cut, T = 0.5 mm, CWL = 435 nm, FWHM = 10 nm; **F**, C-cut, T = 0.5 mm, CWL = 532 nm, FWHM = 0.6 nm; **G**, C-cut, T = 1 mm, FWHM = 200 nm (white light source); **H**, C-cut, T = 1 mm, CWL = 532 nm, FWHM = 30 nm; **I**, C-cut, T = 1 mm, CWL = 532 nm, FWHM = 0.6 nm; **J**, C-cut, T = 2 mm, CWL = 532 nm, FWHM = 30 nm; **K**, C-cut, T = 2 mm, CWL = 630 nm, FWHM = 10 nm; **L**, C-cut, T = 2 mm, CWL = 435 nm, FWHM = 10 nm.

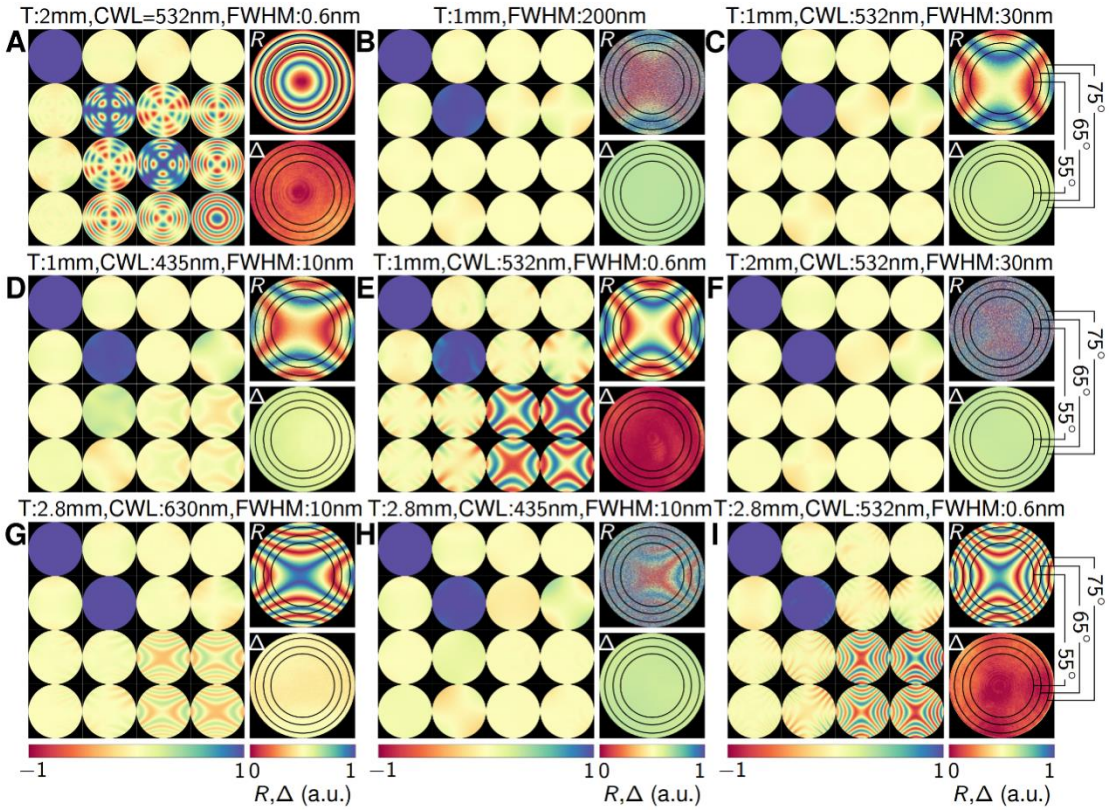

Figure S4. Polarization effects of the conventional endoscope depending on the key factors - full results (part II). Mueller matrices and retardance and depolarization images of the experimental endoscope when the sapphire window mounted at the distal end and the illumination light were: **A**, C-cut, T = 2 mm, CWL = 532 nm, FWHM = 0.6; **B**, A-cut, T = 1 mm, FWHM = 200 nm (white light source); **C**, A-cut, T = 1 mm, CWL = 532 nm, FWHM = 30 nm; **D**, A-cut, T = 1 mm, CWL = 435 nm, FWHM = 10 nm; **E**, A-cut, T = 1 mm, CWL = 532 nm, FWHM = 0.6 nm; **F**, A-cut, T = 2 mm, CWL = 532 nm, FWHM = 30 nm; **G**, A-cut, T = 2.8 mm, CWL = 630 nm, FWHM = 10 nm; **H**, A-cut, T = 2.8 mm, CWL = 435 nm, FWHM = 10 nm; **I**, A-cut, T = 2.8 mm, CWL = 532 nm, FWHM = 0.6 nm

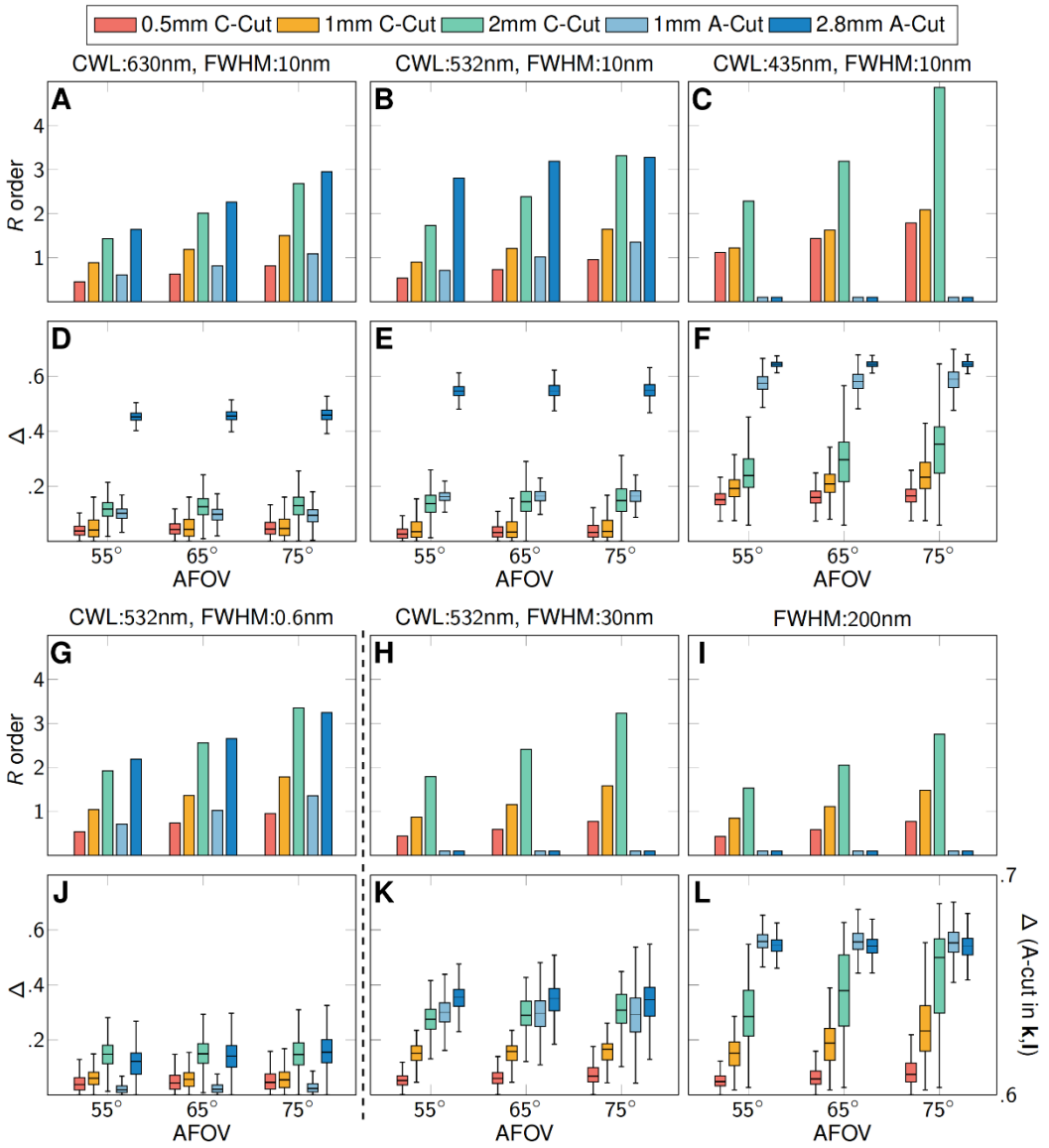

Figure S5. Polarization effects of the conventional endoscope depending on the key factors - full results (part III). Barcharts of the retardance order (*R* order) and boxplots of the depolarization (Δ) of the experimental endoscope depending on the AFOV when various sapphire windows were mounted at the distal end and illuminated by light sources with: CWL = 630 nm, FWHM = 10 nm (**A**,**D**); CWL = 532 nm, FWHM = 10 nm (**B**,**E**); CWL = 435 nm, FWHM = 10 nm (**C**,**F**); CWL = 532 nm, FWHM = 0.6 nm (**G**,**J**); CWL = 532 nm, FWHM = 30 nm (**H**,**K**); FWHM = 200 nm (white light source, **I**,**L**).

4. Birefringence of the sapphire and MgF_2 crystal in visible band

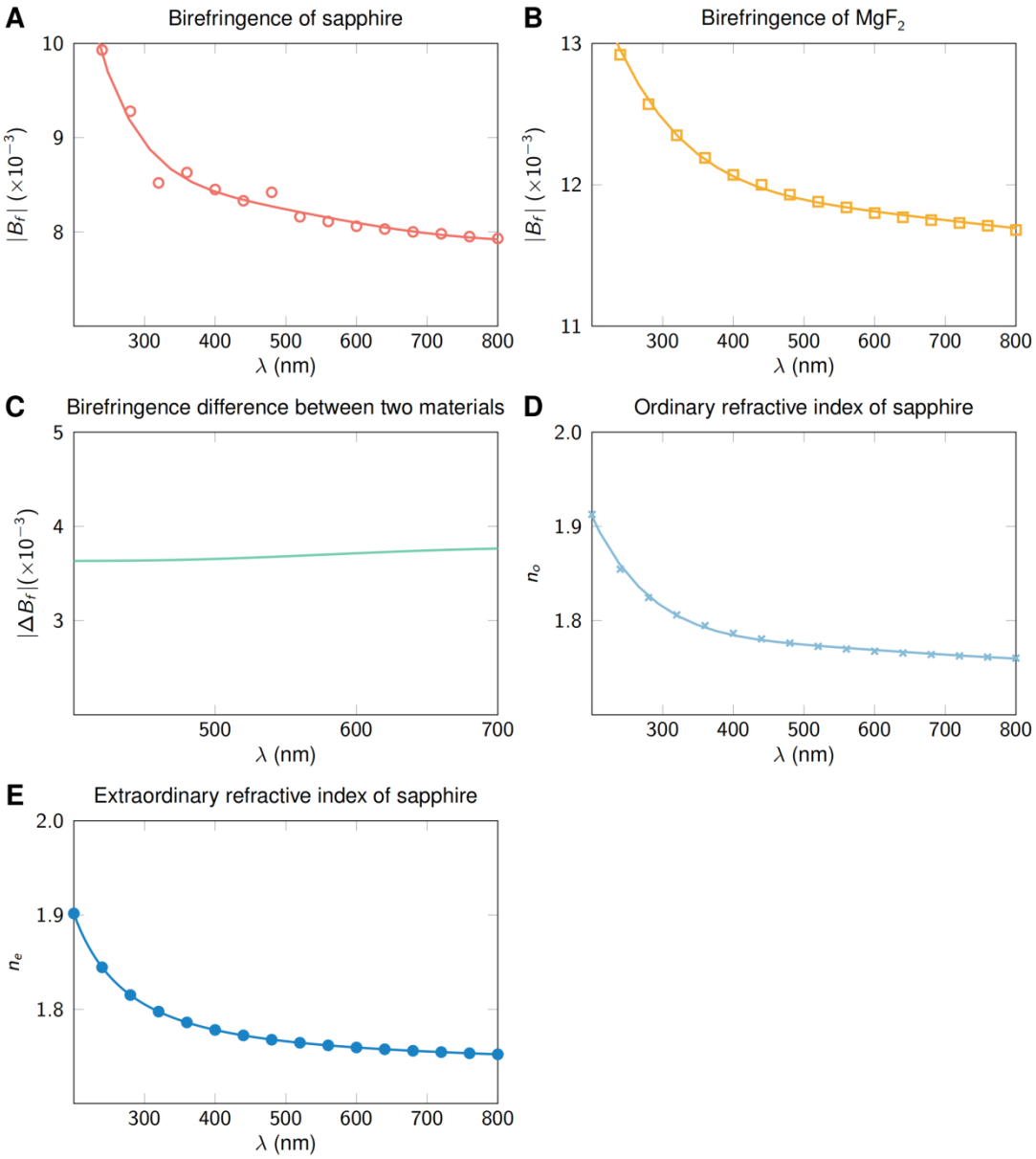

Figure S6. Birefringence of the sapphire and MgF_2 crystals. **A**, The fitted birefringence of the sapphire crystal depend on wavelength. **B**, The fitted birefringence of the MgF_2 crystal depend on wavelength. **C**, The birefringence difference between sapphire and MgF_2 in the visible spectrum. **D**, The fitted ordinary refractive index of the sapphire crystal. **E**, The fitted extraordinary refractive index of the sapphire crystal.

The birefringence curves of the sapphire and MgF_2 crystal fitted with data provided by previous studies[14],[15] in MATLAB 2022b environment. For the birefringence (B_f), here we used the absolute value of the birefringence ($|B_f| = |n_e - n_o|$) for convenient

comparison of the two types of crystals. The specific values of the graphs in Figure S6 can be found in the source data file.

5. Polarization effects of the conventional endoscope illuminated by light source with various bandwidths

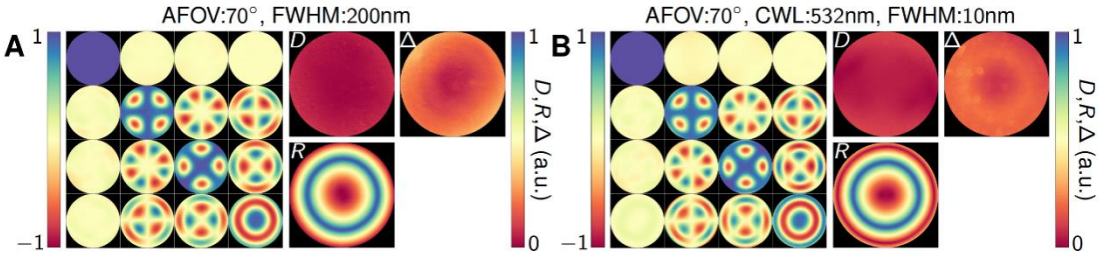

Figure S7. Polarization effects of the conventional endoscope (J0800B, ShenDa) illuminated by light sources with various bandwidths. The light sources include: **A**, the white light source (FWHM = 200 nm); **B**, the green LED light source (CWL = 532 nm, FWHM = 30 nm); and **C**, the narrowband light source (CWL = 532 nm, FWHM = 10 nm).

6. Specular highlight removal with computation-based methods

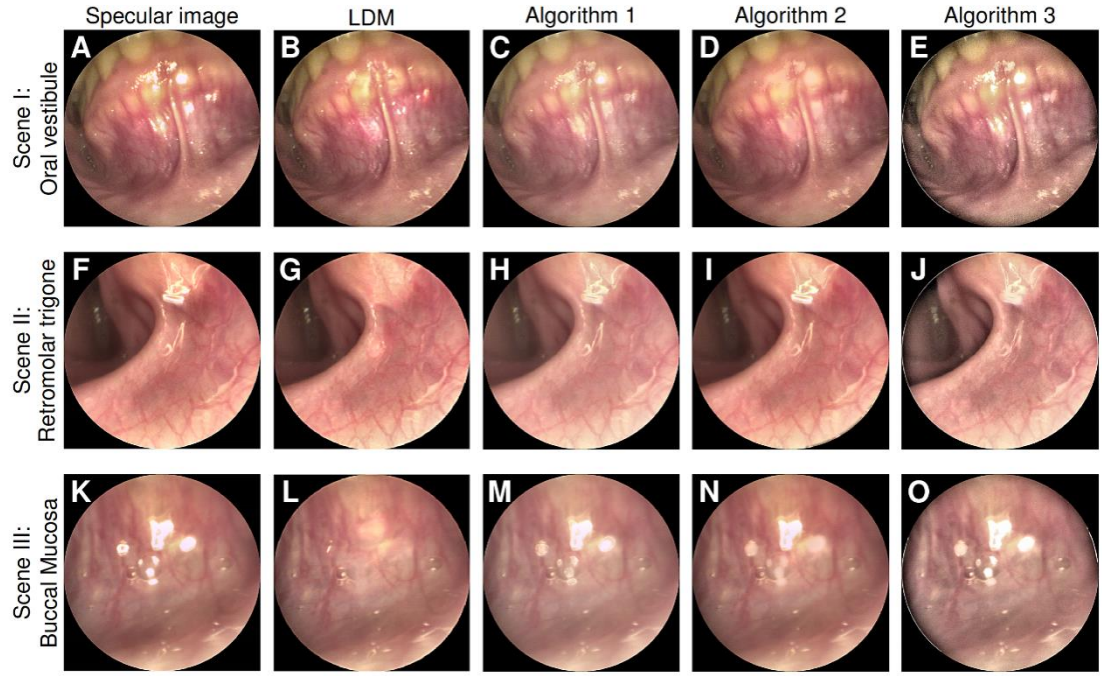

Figure S8. Specular highlight removal results with computation-based methods. A,**F**,**K**, The specular WLE images of the oral vestibule, retromolar trigone and Buccal Mucosa. **B**,**G**,**L**, The corresponding specular highlight removed images processed with the LDM algorithm. **C**,**H**,**M**, The

corresponding specular highlight removed images processed with algorithm 1. **D**,**I**,**N**, The corresponding specular highlight removed images processed with algorithm 2. **E**,**J**,**O**, The corresponding specular highlight removed images processed with algorithm 3.

To compare our PG-WLE with computation-based methods for specular highlight removal, we firstly compared several computation-based methods and chose the representative method. In this work, the compared algorithms include the LDM[16], the enhanced fast marching inpainting method[17] (referred to as algorithm 1), the dichromatic reflection model-based multi-resolution inpainting method[18] (referred to as algorithm 2) and the retinex image enhancement based specular highlight removal methods[19] (referred to as algorithm 3).

7. Full results of the polarimetric endoscopy with the polarization film targets

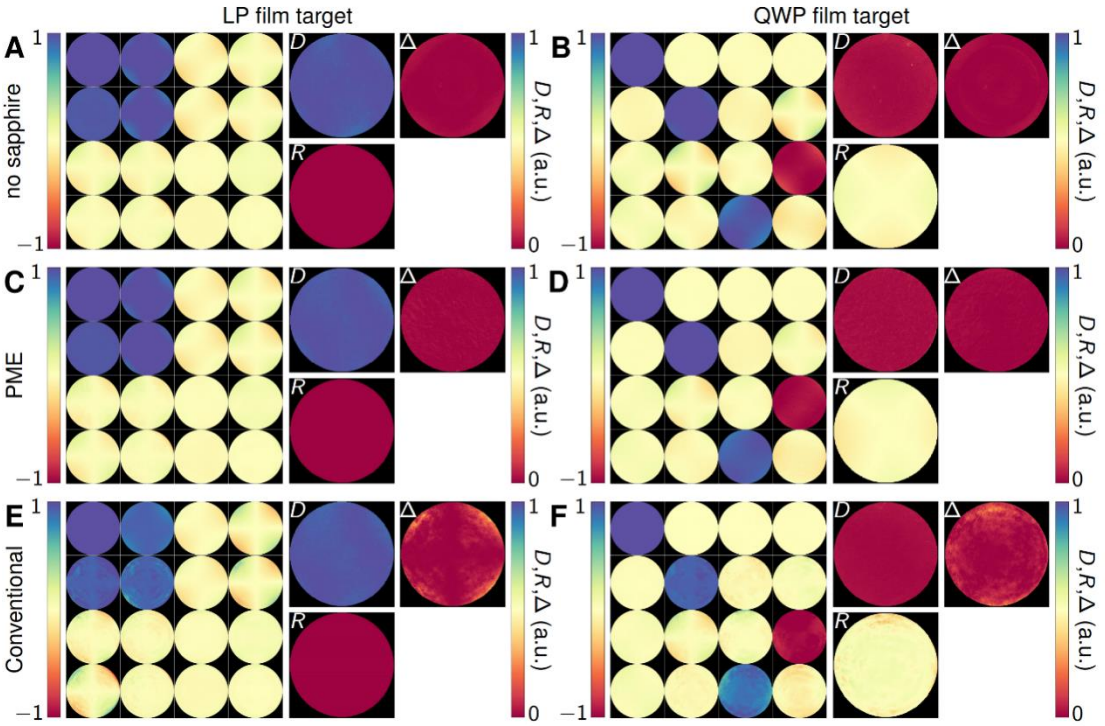

Figure S9. Full results of the polarimetric endoscopy with polarization film targets. A-B, The LP film target (**A**) and the quarter waveplate (QWP) film target (**B**) imaged by the endoscopic Mueller polarimetric imaging system with the experimental endoscope without sapphire windows. **C-D**, LP (**C**) and QWP (**D**) film targets imaged with the PME. **E-F**, LP (**E**) and QWP (**F**) film targets imaged with the conventional endoscope (J0800B, ShenDa).

8. Full results of the polarimetric endoscopy with *ex vivo* tissue

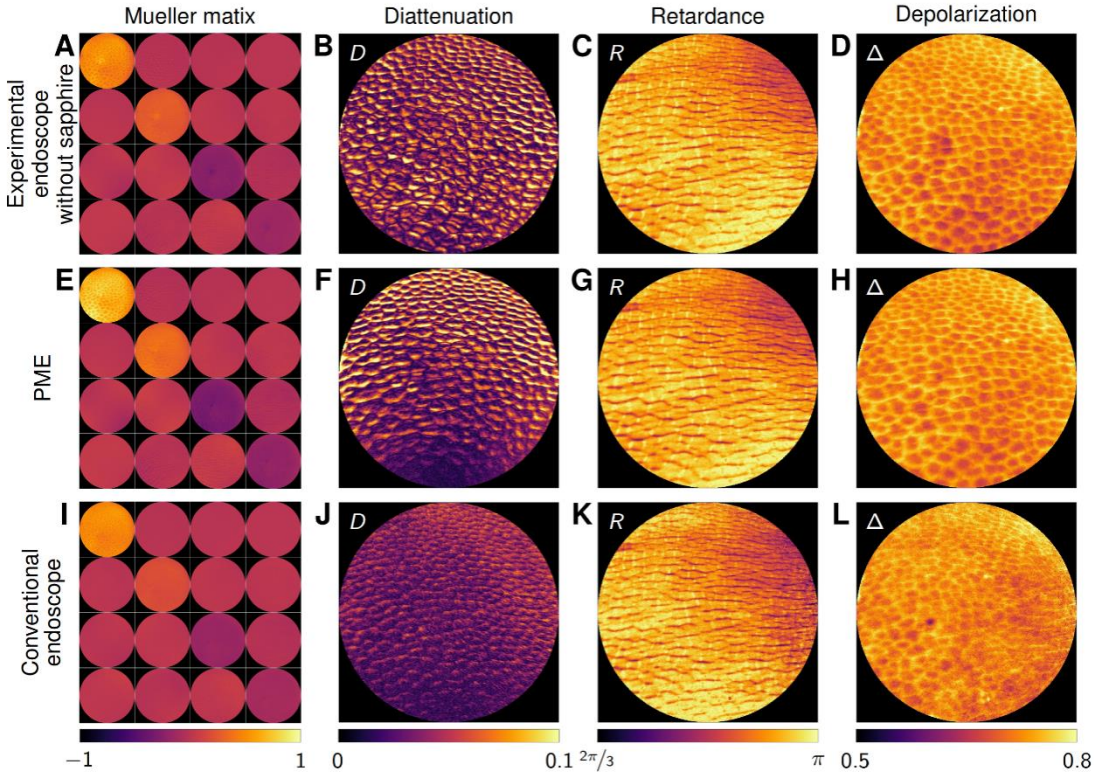

Figure S10. Full results of the polarimetric endoscopy with the *ex vivo* porcine liver tissue. A-D, Mueller matrix (**A**) and diattenuation (**B**), retardance (**C**) and depolarization (**D**) images obtained by the endoscopic Mueller imaging system with experimental endoscope without sapphire windows. **E-H**, Mueller matrix (**E**) and diattenuation (**F**), retardance (**G**) and depolarization (**H**) images obtained with the PME. **I-L**, Mueller matrix (**I**) and diattenuation (**J**), retardance (**K**) and depolarization (**L**) images obtained with the conventional endoscope (J0800B, ShenDa).

9. Full results of the polarimetric endoscopy with oral cavity *in vivo*

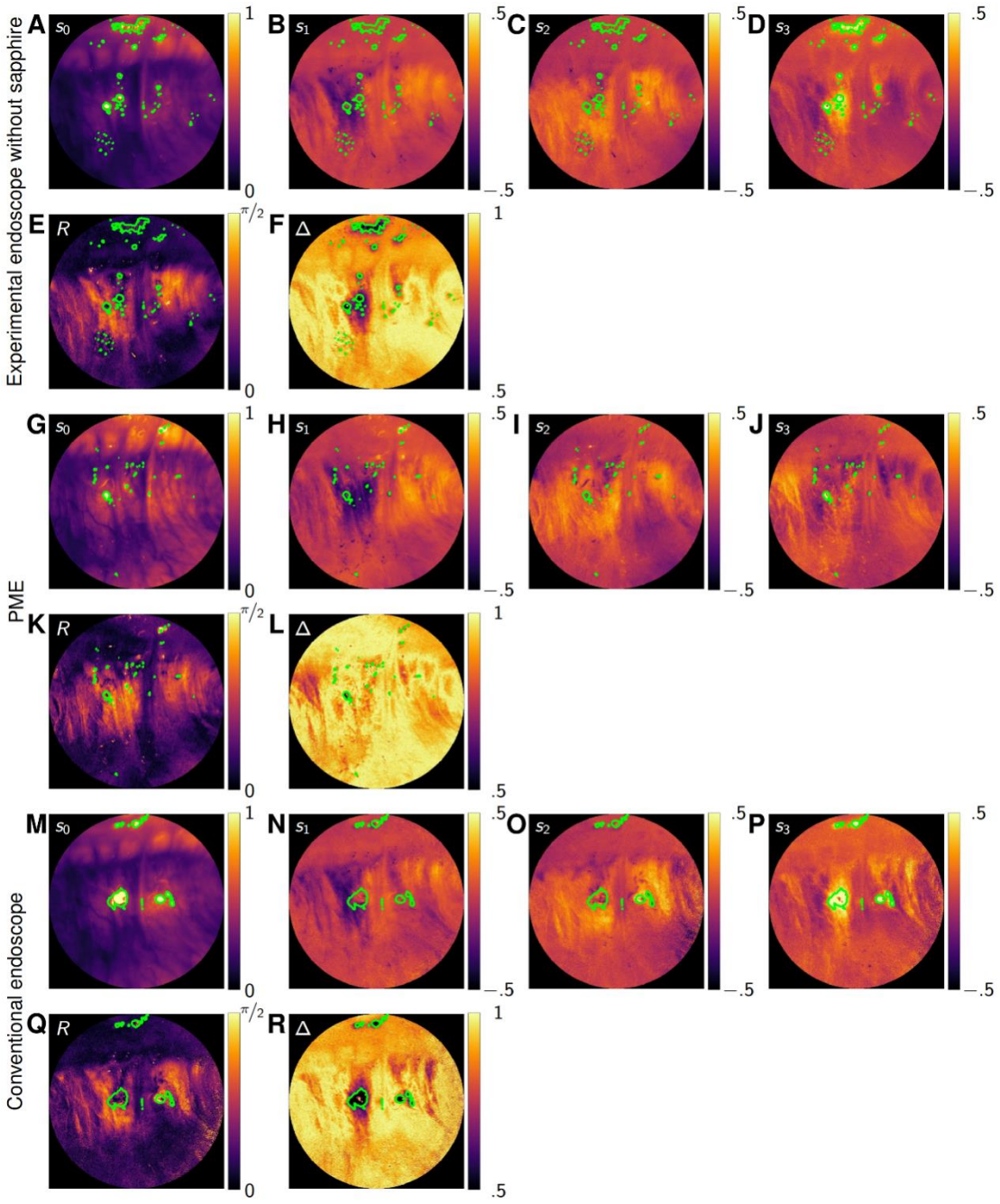

Figure S11. Full results of the polarimetric endoscopy with oral cavity *in vivo*. **A-F**, The Stokes parameter (s_0-s_3, **A-D**), retardance (**E**) and depolarization (**F**) images of the oral vestibule obtained by the snapshot endoscopic Stokes imaging system with the experimental endoscope without sapphire windows. **G-L**, s_0-s_3 (**G-J**), retardance (**K**) and depolarization (**L**) images obtained with the PME. **M-R**, s_0 - s_3 (**M-P**), retardance (**Q**) and depolarization (**R**) images obtained with the conventional endoscope. The green lines in the image circle out the invalid specular highlight areas.

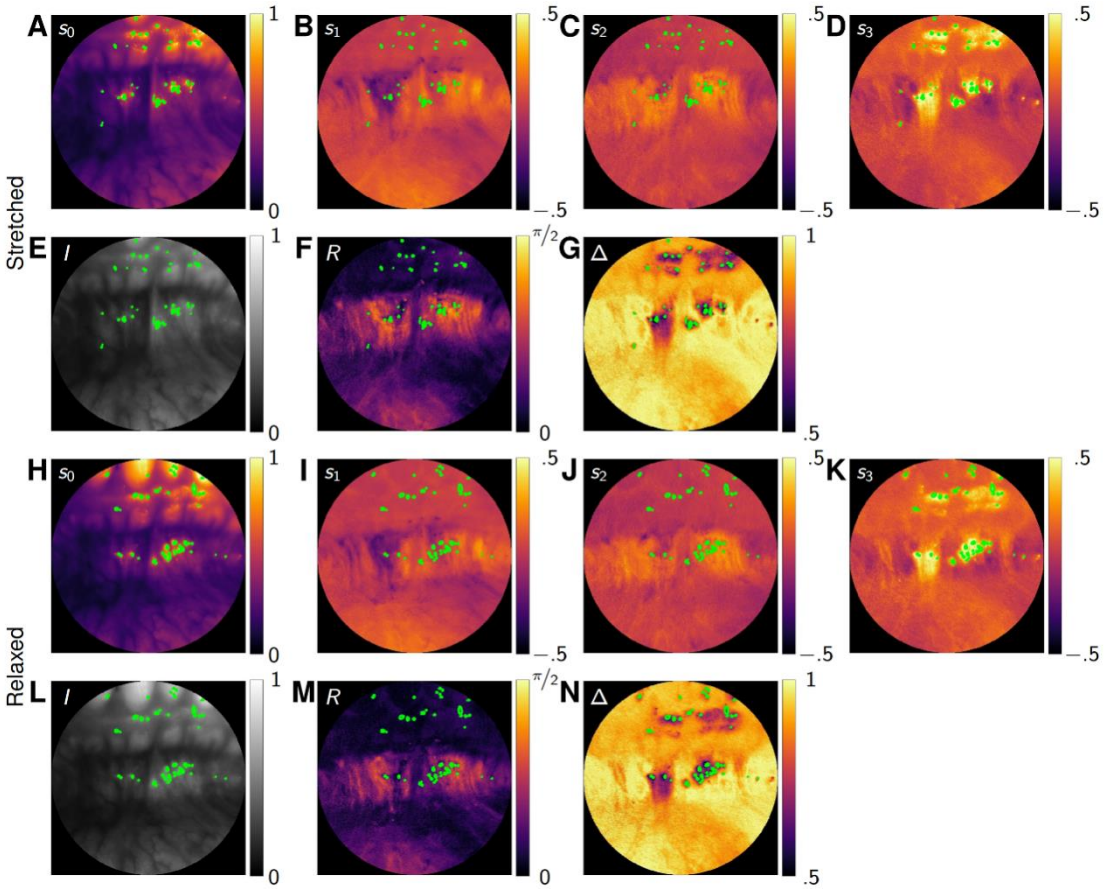

Figure S12. Full results of the polarization properties of the oral vestibule obtained by the snapshot endoscopic Stokes imaging system with the PME when it is stretched and relaxed. A-G, s_0-s_3 (**A-D**), intensity (**E**), retardance (**F**) and depolarization (**G**) images of the stretched oral vestibule. **H-N**, s_0-s_3 (**H-K**), intensity (**L**), retardance (**M**) and depolarization (**N**) images of the relaxed oral vestibule. The green lines in the image circle out the invalid specular highlight areas.

10. Benchtop Mueller imaging system setup

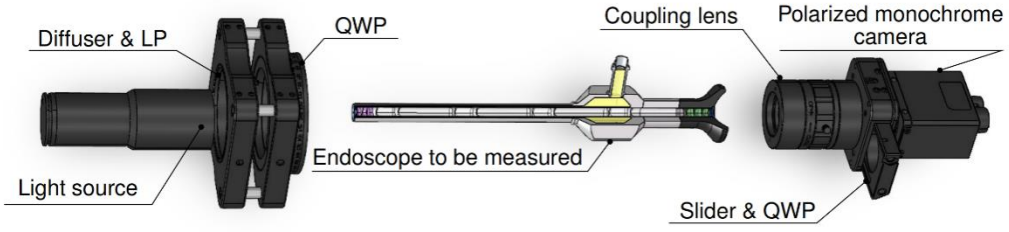

Figure S13. The benchtop Mueller polarimetric imaging system setup.

11. Endoscopic polarimetric imaging error depending on the depolarization of the

endoscope

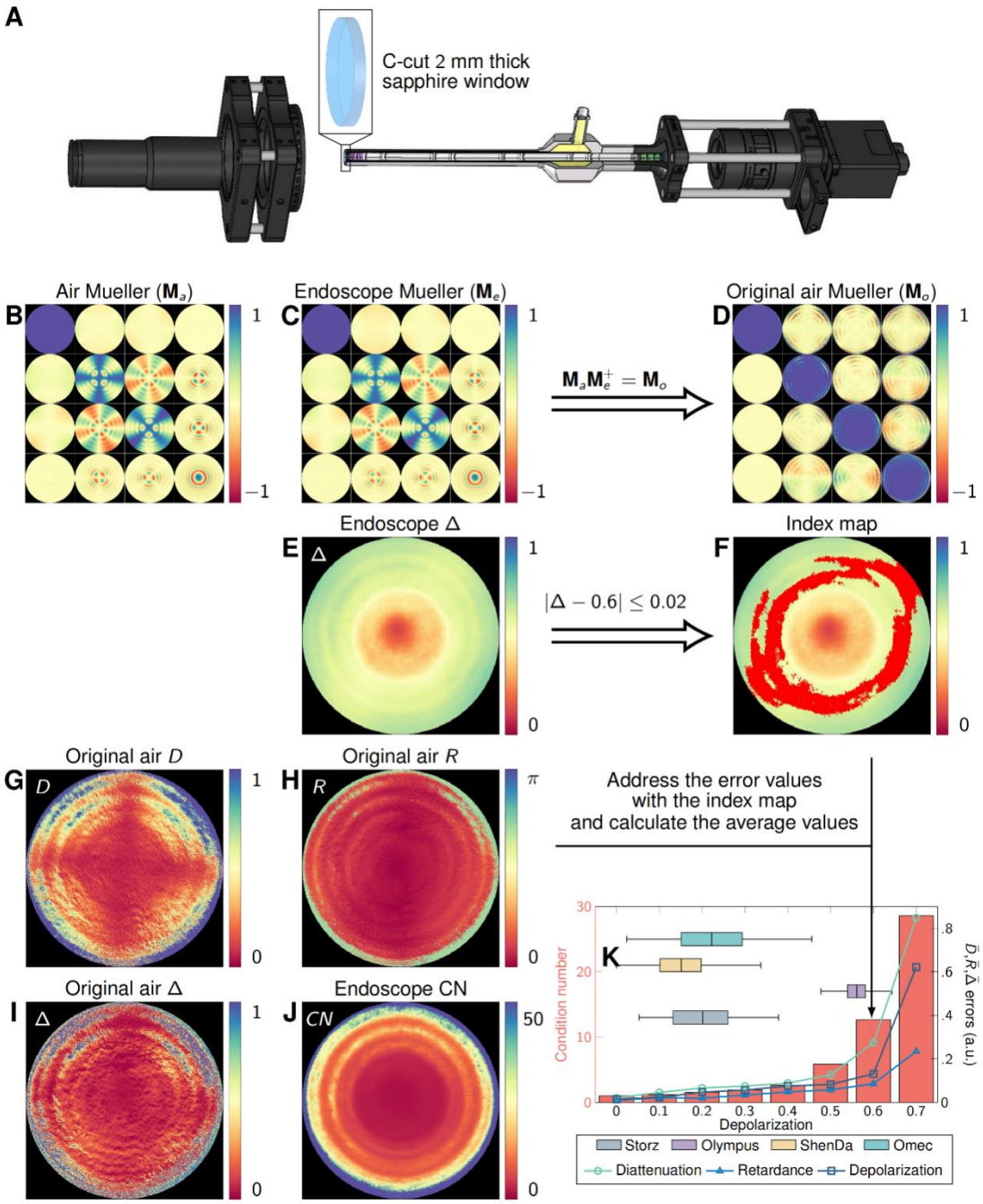

Figure S14. The endoscopic polarimetric imaging error depending on the level of depolarization of the endoscope. A, The system setup for the experiment. **B**, The Mueller matrix of the air ($\mathbf{M}_a$) measured by the endoscopic Mueller imaging system. **C**, The Mueller matrix of the experimental endoscope ($\mathbf{M}_e$) measured by the benchtop Mueller imaging system. **D**, The reconstructed original Mueller matrix of the air ($\mathbf{M}_o$). **E**, the depolarization image of the endoscope. **F**, An index map example (red dots indicate points where depolarization are close to 0.6) calculated from the depolarization image of the conventional endoscope. **G-I**, The diattenuation, retardance and depolarization images calculated from the original

Mueller matrix of the air ($\mathbf{M}_o$). **J**, the condition number (CN) image of the conventional endoscope. **K**, Graph of CN and errors in the reconstructed diattenuation, retardance and depolarization depending on the depolarization of the endoscope.

To obtain the endoscopic Mueller imaging error depending on the depolarization of the endoscope, we measured the Mueller matrix of the air ($\mathbf{M}_a$, Figure S14B) using the endoscopic polarimetric imaging system with the experimental endoscope. The system setup is present in Figure S14A. The endoscope had the 2 mm C-cut sapphire window mounted on the distal end and the AFOV is restricted to $70°$, and the white light source is adopted in the PSG of the system. To reconstruct the original Mueller matrix of the air, we also measured the Mueller matrix of the endoscope ($\mathbf{M}_e$, Figure S14C) with the benchtop Mueller imaging system. The original Mueller matrix of the air ($\mathbf{M}_o$, Figure S14D) was then calculated by

$$\mathbf{M}_o = \mathbf{M}_a\mathbf{M}_e^+$$

Since the depolarization of the endoscope with the C-cut sapphire window in the FOV is radially increased (Figure S14E), the measurement error with the increasing depolarization can be obtained within the FOV of the experimental endoscope. Therefore, we calculated the index map (Figure S14F) from the depolarization image of the endoscope that labels the points with depolarization close to 0, 0.1, 0.2, …, 0.7 (within ± 0.02). With the index map, we then address the corresponding values in the diattenuation (Figure S14G), retardance (Figure S14H) and depolarization (Figure S14I) images decomposed from the original Mueller matrix of the air and the CN image of the endoscope (Figure S14J). The final results were then obtained by calculating the average value of the addressed data.

12. Angular setup in the simulation study

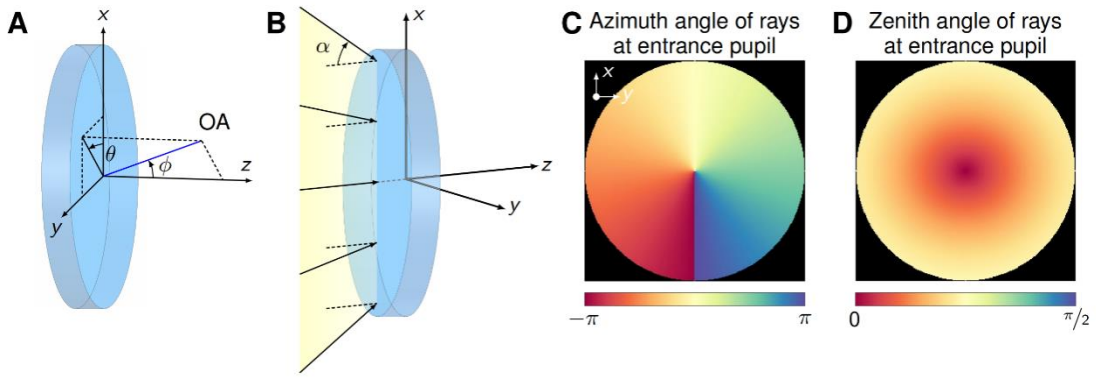

Figure S15. Angular setup for the OA and rays in the simulations. A, The azimuth (θ) and zenith (ϕ) angle describing the OA direction of the sapphire window. **B**, The direction of the incident primary rays depending on the AFOV of the endoscope. **C**, Azimuth angle of the rays at the entrance pupil. **D**, Zenith angle of rays at entrance pupil.

In the simulation, we assumed the surface normal of the sapphire window to be along the *z*-axis direction and defined the direction of the OA and rays by their zenith angle (ϕ, Figure S15A) with respect to the *z*-axis and the azimuth angle in *x*-*o*-*y* plane with respect to *x*-axis (θ, Figure S15A). The AFOV of the endoscopes was assumed as $80°$ and the primary rays thus had a zenith angle of $40°$ at the edge of the FOV (zenith angle α=AFOV/2). For the entire field of the incident primary rays, their incident directions were set with azimuth angles rotating around the z-axis and zenith angles varying from $0°$ to $35°$ from the center of the field to the edge.

13. Spectra of the light sources

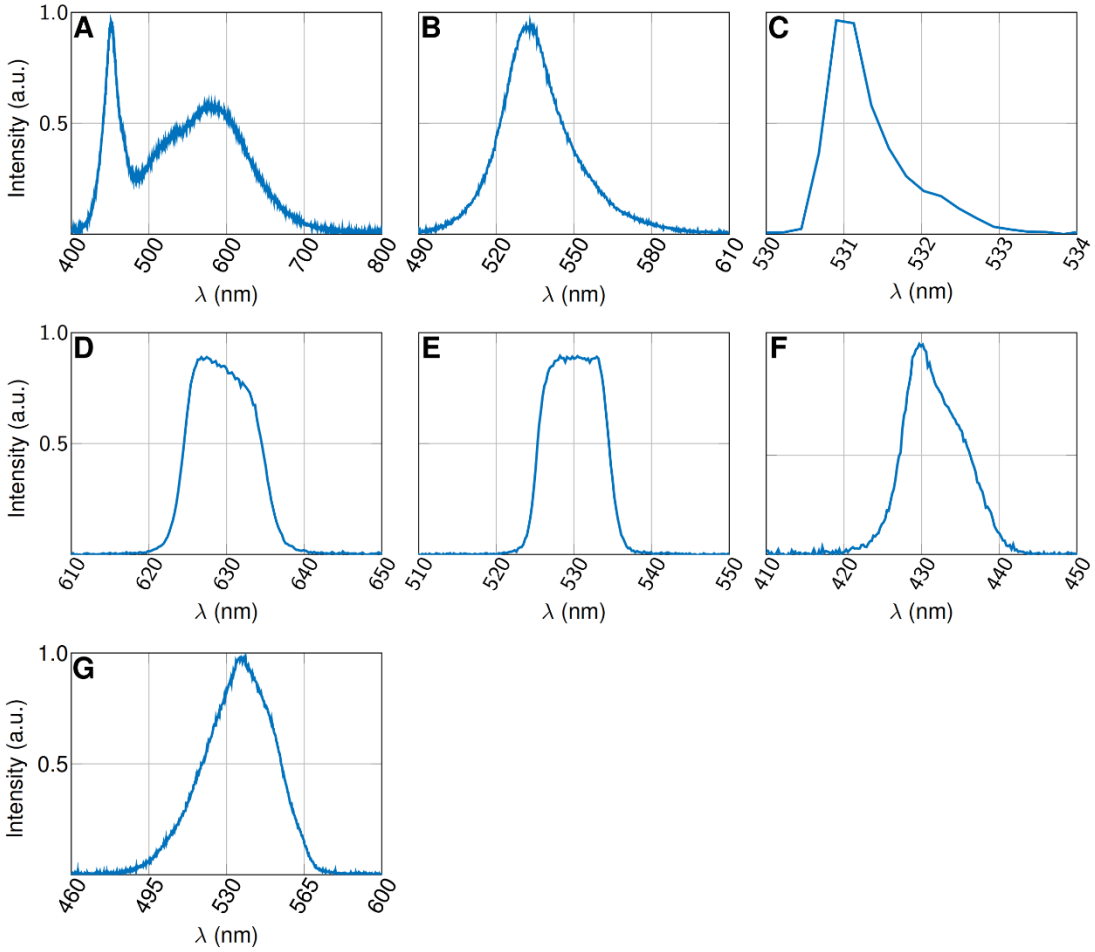

Figure S16. The spectra of light sources used in this study. The light sources include: **A**, The white light source (LED-D1-MAX6K, Oeabt); **B**, the green LED light source (HI-080, HengYang); **C**, the single longitudinal mode laser (opus 532, Novanta Photonics); **D-E**, the narrowband light sources constructed by the white light source and the bandpass filer BP630-10nm (**D**), BP532-10nm (**E**), BPH435-10nm (**F**); and **G**, the endoscopic cold light source (RFFM-16A5, Rayfine).

14. Endoscopic polarization-gated imaging system setup

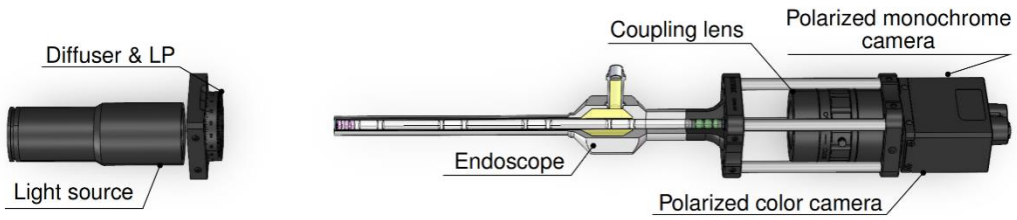

Figure S17. The endoscopic polarization-gated imaging system setup.

15. Endoscopic Mueller polarimetric imaging system setup

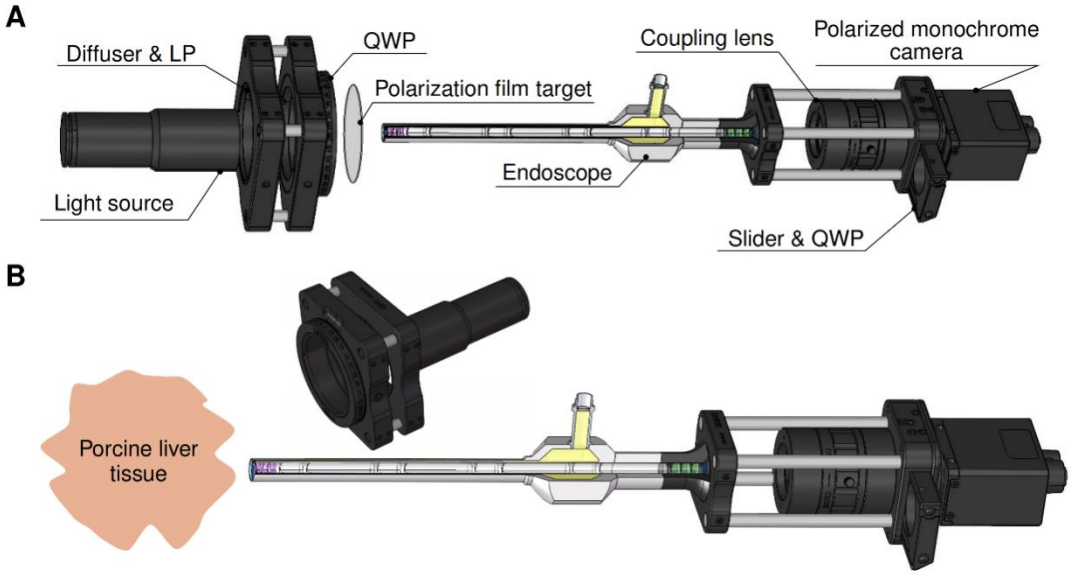

Figure S18. The endoscopic Mueller polarimetric imaging system setup. The system is operated in the transmission mode to measure the polarization properties of the polarization targets (**A**), and in the reflection mode to measure the *ex vivo* porcine liver (**B**).

16. The snapshot endoscopic Stokes imaging system

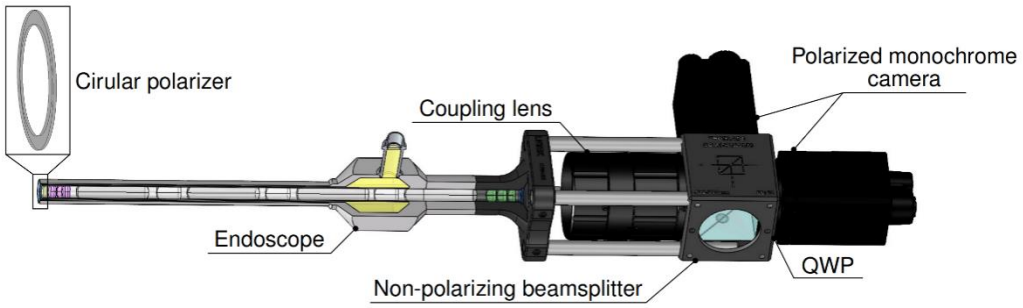

Figure S19. The snapshot endoscopic Stokes imaging system setup.

References

[1] Liang, R. Optical design for biomedical imaging (SPIE, 2010).+

[2] Lu, S-Y. & Chipman, R. A. Interpretation of Mueller matrices based on polar decomposition. *J. Opt. Soc. Am. A.* **13**, 1106-1113 (1996).

[3] Qi, J. & Elson, D. S. (2016). A high definition Mueller polarimetric endoscope for tissue characterisation. Sci. Rep. 6, 25953. https://doi.org/10.1038/srep25953

[4] Avendaño-Alejo, M. and Stavroudis, O. N. (2002). Huygens's principle and rays in uniaxial anisotropic media. II. Crystal axis orientation arbitrary. JOSA A, 19, 1674-1679. https://doi.org/10.1364/JOSAA.19.001674

[5] Born, M. & Wolf, E. (2013). Principles of optics: electromagnetic theory of propagation, interference and diffraction of light (Elsevier Press)

[6] Chipman, R., Lam, W. S. T. & Young, G. (2018). Polarized light and optical systems (CRC Press)

[7] Malitson, I. H. (1962). Refraction and dispersion of synthetic sapphire. J. Opt. Soc. Am., 52, 1377-1379. https://doi.org/10.1364/JOSA.52.001377

[8] Ambirajan, A. & Look, Jr. D. C. (1995). Optimum angles for a polarimeter: part I. Opt. Eng. 34, 1651-1655. https://doi.org/10.1117/12.202093

[9] Macias-Romero, C. & Török, P. (2012). Eigenvalue calibration methods for polarimetry. J. Eur. Opt. Soc. Rapid Publ. 7. https://doi.org/10.2971/jeos.2012.12004

[10] Li R., Pan J., Si Y., Yan B., Hu Y., Qin H. (2019). Specular reflections removal for endoscopic image sequences with adaptive-RPCA decomposition. IEEE trans. Med. Imaging 39, 328-340. https://doi.org/10.1109/TMI.2019.2926501

[11] Wang, D., Song, J., Gao, J., Qi, J. & Elson, D. S. (2024). Computational polarization imaging in vivo through surgical smoke using refined polarization difference. Adv. Sci. 11 (30). https://doi.org/10.1002/advs.202309998

[12] Venkatanath, N., Praneeth, D., Bh, M. C., Channappayya, S. S. and Medasani, S. S. (2015). Blind image quality evaluation using perception based features. NCC-2015, IEEE, 1-6. https://doi.org/10.1109/ncc.2015.7084843

[13] Qi, J., Tatla, T., Nissanka-Jayasuriya, E., Yuan, A. Y., Stoyanov, D., Elson, D. S. (2023). Surgical polarimetric endoscopy for the detection of laryngeal cancer. Nat. Biomed. Eng. 7, 971-985. https://doi.org/10.1038/s41551-023-01018-0

[14] Malitson, I. H. (1962). Refraction and dispersion of synthetic sapphire. JOSA, 52, 1377-1379. https://doi.org/10.1364/JOSA.52.001377

[15] Dodge, M. J. (1984). Refractive properties of magnesium fluoride. Appl. Opt., 23, 1980-1985. https://doi.org/10.1364/ao.23.001980

[16] Rombach R., Blattmann A., Lorenz D., Esser P., Ommer B. (2022). High-resolution image synthesis with latent diffusion models. Proc. IEEE/CVF Conf. Comput. Vis. Pattern Recognit., 10684-10695. https://doi.org/10.1109/cvpr52688.2022.01042

[17] Tchoulack, S., Langlois, J. P. and Cheriet, F. (2008). A video stream processor for real-time detection and correction of specular reflections in endoscopic images. 2008 Joint IEEE-NEWCAS and TAISA, 49-52. https://doi.org/10.1109/newcas.2008.4606318

[18] El Meslouhi, O., Kardouchi, M., Allali, H., Gadi, T. and Benkaddour, Y. A. (2011). Automatic detection and inpainting of specular reflections for colposcopic images. Cent. Eur. J. Comput. Sci., 1, 341-354. https://doi.org/10.2478/s13537-011-0020-2

[19] Rahman, Z. U., Jobson, D. J. and Woodell, G. A. (2004). Retinex processing for automatic image enhancement. J. Electron. Imaging, 13, 100-110. https://doi.org/10.1117/1.1636183